W&M ScholarWorks

Undergraduate Honors Theses

Theses, Dissertations, & Master Projects

4-2018

Characterizing the Intracellular Distribution of Mutant Thyroid Hormone Receptor α-1 A382PfsX7

Kristin Passero

Follow this and additional works at: https://scholarworks.wm.edu/honorstheses

Part of the Cell Biology Commons, and the Molecular Genetics Commons

Recommended Citation

Passero, Kristin, "Characterizing the Intracellular Distribution of Mutant Thyroid Hormone Receptor α-1 A382PfsX7" (2018). *Undergraduate Honors Theses*. Paper 1187.
https://scholarworks.wm.edu/honorstheses/1187

This Honors Thesis is brought to you for free and open access by the Theses, Dissertations, & Master Projects at W&M ScholarWorks. It has been accepted for inclusion in Undergraduate Honors Theses by an authorized administrator of W&M ScholarWorks. For more information, please contact scholarworks@wm.edu.

Characterizing the Intracellular Distribution of Mutant Thyroid Hormone Receptor α-1 A382PfsX7

A thesis submitted in partial fulfillment of the requirement for the degree of Bachelor of Science with Honors in Biology from the College of William and Mary

Kristin Passero

Accepted for Honors

Dr. Lizabeth Allison (Advisor)

Dr. Shantá Hinton

Professor John Lee

Professor Nicole M. Santiago

Dr. Diane Shakes

Williamsburg, VA
30 April 2018

Characterizing the Intracellular Distribution of Mutant Thyroid Hormone Receptor α-1 A382PfsX7

TABLE OF CONTENTS

Table of Contents 3
Abstract 5
INTRODUCTION 6
The Hypothalamic-Pituitary-Thyroid Axis 6
Thyroid Hormone Transport and Processing 7
Thyroid Hormone Receptors 8
Thyroid Hormone Receptor Domains 9
Intracellular Trafficking of Thyroid Hormone Receptors 10
TR Regulation of Gene Expression 11
Role of Thyroid Hormone Signaling in Development and Disease 13
Resistance to Thyroid Hormone Syndrome 15
TRα1 Mutant A382PfsX7 16
Investigation of the Intracellular Localization of Mutant A382PfsX7 17
EXPERIMENTAL DESIGN 18
Construction of Recombinant Protein mCherry-A382PfsX7 Plasmid 18
Cell Culture and Transfection 19
Localization Assay Scoring and Analysis 20
Aggregation Assay Scoring and Analysis 20
RESULTS 21
Coexpression of WT-TRα1 and A382PfsX7 Increases Cytosolic Distribution 21
Table 1: Localization of A382PfsX7 and WT-TRα1 23
Co-transfection of WT-TRα1 and A382PfsX7 Shows Increased Presence of TR Aggregates 23
Table 2: Comparison of TR Aggregation Across Treatments 25
Table 3: Magnitude of Aggregation 25
DISCUSSION 26
Localization and the Dominant-Negative Effect of A382PfsX7 26
WT/A382PfsX7 Coexpression and Aggregate Formation 28
Implications of Aggregation on RTH Therapeutic Practices 31
References 33
Figure 1: Hypothalamic-Pituitary-Thyroid Axis 38
Figure 2: Forms of Thyroid Hormone 39
Figure 3: Thyroid Hormone Transport 40

Figure 4: Thyroid Hormone Receptor Nucleocytoplasmic Transport 41
Figure 5: Regulation of Thyroid Hormone Receptor at Response Elements 42
Figure 6: Domains of TRα1 and A382PfsX7 43
Figure 7: Experimental Methodology 44
Figure 8: Localization of WT-TRα1 and A382PfsX7 45
Figure 9: Localization of WT-TRα1 and Co-Transfected WT 46
Figure 10: Localization of A382PfsX7 and Co-Transfected A382PfsX7 47
Figure 11: Localization Assay Images 48
Figure 12: Presence of A382PfsX7 and WT-TRa1 Aggregates in Co-Transfected HeLa cells 49
Table 4: N:C Ratio Data 50
Table 5: Chi-Square Observed Frequencies 51

ABSTRACT

Resistance to Thyroid Hormone (RTH) syndrome is a developmental disease characterized by the failure of peripheral tissues to respond to thyroid hormone signaling. A382PfsX7 is a nonfunctional RTH-associated variant of thyroid hormone receptor α1 which fails to bind thyroid hormone and disassociate from corepressors. The mutation also deletes a nuclear export signal (NES) from the C-terminal end of the receptor. This thesis sought to determine whether this NES deletion altered the intracellular distribution of TR in a way which would imply interference with its role in transcriptional activation and repression. Using lipid-based transfection of fluorescently-labeled TR into HeLa (human) cells and fluorescent microscopy, the nuclear-to-cytoplasmic ratio of wild-type (WT) and mutant TR and the presence of TR aggregates was evaluated. Coexpression of WT-TRα1 and A382PfsX7 is associated with a cytosolic shift in localization and an increased frequency of TR aggregation. These data suggest that novel interactions between WT and mutant receptors may increase the aggregation propensity of TR and thereby alter localization.

INTRODUCTION

In response to developmental or environmental cues, hormones are released into the blood and travel to peripheral tissues, where they bind receptors and elicit developmental and metabolic changes. One such ligand-receptor pair is thyroid hormone (TH) and the thyroid hormone receptor (TR). There are multiple checkpoints which regulate thyroid hormone signaling and mutations or exogenous disruptions at any of these checkpoints could dysregulate the system. This thesis studies the intracellular localization of a mutant form of thyroid hormone receptor alpha 1 (TRα1) that causes the disorder Resistance to Thyroid Hormone syndrome.

The Hypothalamic-Pituitary-Thyroid Axis

Production of TH begins with the secretion of thyrotropin-releasing hormone (TRH) from the hypothalamus (Figure 1). TRH is received by TRH receptors on the anterior pituitary gland. In response to the TRH signal, the pituitary gland produces and secretes thyrotropin/thyroid-stimulating hormone (TSH) which in turn stimulates the thyroid gland.

Thyroid hormone is synthesized in the follicular cells and the follicular lumen of the thyroid gland (Mondal et al., 2016). Iodine is transported into the follicles via the sodium iodine symporter. An unknown iodide transporter moves I^- from the follicular thyroid cells into the lumen where TH biosynthesis occurs (Mondal et al., 2016). Thyroid peroxidase (TPO), in the presence of hydrogen peroxide, catalyzes the iodination of tyrosine residues on homodimeric thyroglobin (Tg) (Yen et al., 2001; Mondal et al., 2016). TPO also facilitates the phenolic coupling of iodinated tyrosyls on Tg (Mondal et al., 2016). Although Tg is abundant in the thyroid follicles, each Tg produces only one to four TH molecules, due to less than 3% of its tyrosine residues being properly accessible for iodination. The iodinated tyrosyls remain bound to Tg and are stored in the follicular lumen (Yen et al., 2001; Mondal et al., 2016). Continuing

production and secretion of TSH from the anterior pituitary induces the proteolysis of the coupled tyrosyls from Tg, releasing TH for transport (Mondal et al., 2016). Monocarboxylate transporter 8 (MCT8), a high-affinity transporter for T_4 and T_3, exports TH into the blood serum (Halestrap, 2012).

T_4 and T_3 differ in their pattern of iodination and their affinity for TR (Figure 2). In T_4, both carbon rings are di-iodinated; in contrast, the outer ring of T_3 is mono-iodinated. T_3 is the major TR ligand, although T_4 can bind TR with lesser affinity. The thyroid gland predominantly makes inactive T_4 but does produce and secrete biologically active T_3 at lesser levels. The majority of T_3 is produced via deiodination of the outer ring of T_4 (Yen et al., 2001). TH biosynthesis is controlled by a negative feedback loop. Elevated levels of circulating TH inhibit the TRH-TSH signaling pathway, decreasing TH production.

Thyroid Hormone Transport and Processing

Due to its general hydrophobic nature, TH binds to several transport proteins to travel through the blood serum (Figure 3). Thyroxine-binding globulin (TBG), transthyretin (TTR), and human serum albumin (HSA) all play a role in the transport of TH to peripheral tissues (Mondal et al., 2016; Yen et al 2001). While TBG has the highest affinity for T_4, TTR and HSA have higher plasma concentrations, giving them a general binding capacity greater than that of TBG (Mondal et al., 2016). However, cells only uptake free T_4 and T_3 (Yen et al., 2001). TH bound to serum transport proteins cannot enter peripheral tissues, but this interaction with transport proteins is impermanent. Eventual dissociation of TH allows for its uptake by peripheral tissues via plasma membrane transporter MCT8.

Inside the cell, T_4 undergoes deiodination to convert it into active T_3. Iodothyronine deiodinases (DIOs) catalyze deiodination of TH. Mono-deiodination of the phenolic outer ring

forms active T_3. Removal of iodine from the inner ring produces inactive rT_3 (Mondal et al., 2016). Further deiodination of T_3 produces another inactive TH variant, T_2. Diffusion of TH into the nucleus and binding to TR results in TR-mediated recruitment of coactivators and other complexes which activate TH-target gene transcription.

Thyroid Hormone Receptors

Thyroid hormone receptors are ligand-activated transcription factors and members of the nuclear receptor (NR) superfamily. Unlike many nuclear receptors, such as steroid receptors, TRs do not require ligand binding to translocate into the nucleus. They regulate transcription by interacting with thyroid hormone response elements (TREs) independent of TH (Yen et al., 2006). Classically, TR positively regulates TREs. Upon ligand binding, TR disassociates from its corepressors and recruits coactivators to begin transcriptional activation (Figure 5). Negatively controlled TREs have also been identified but are poorly characterized.

Two genes encode thyroid hormone receptors. The *THRA* gene, located on chromosome 17, regulates the production of TRα and its subtypes. The other gene, *THRB* located on chromosome 3, codes for TRβ subtypes. Between these two loci, four major TH-binding variants are produced: TRα1, TRβ1, TRβ2, and TRβ3 (Brent 2012; Cheng et al 2010). *THRA* also produces TRα2, a C-terminal variant of TRα which is unable to bind ligand (Liu et al., 1995; Burgos-Trinidad and Koenig 1999; Yen et al., 2006). Although highly conserved in sequence and mechanism of function, these four subtypes regulate different bodily processes through tissue-dependent expression. TRα1 is most highly expressed in skeletal muscle, the gastrointestinal tract, heart, and brain. TRβ1 is in the liver, brain, kidney, and thyroid. TRβ2 is in the anterior pituitary, hypothalamus, and retina. TRβ3 is in the kidney, livers, and lungs (Brent, 2012; Cheng et al., 2010; Mondal et al., 2016). Most notably, this tissue-dependent expression

means TRβ isoforms have a greater role in mediating the negative feedback loop of TH expression.

Thyroid Hormone Receptor Domains

Thyroid hormone receptors consist of four major domains— (1) a variable N-terminal A/B domain, (2) a DNA-binding domain (DBD), (3) a hinge domain, and (4) a ligand-binding domain (LBD). Among the NR superfamily—and between TR subtypes—the A/B domain has the greatest variability in sequence and length (Wu et al., 2000; Jin and Li, 2010; Brent, 2012). It contains activation function-1 (AF-1) (Wu et al., 2000; Jin and Li, 2010). AF-1 induces ligand-independent transactivation. A study of TR-heterodimer function without T_3 stimulation was still able to quantify levels of the β-galactosidase reporter, presumably due to the AF-1-mediated transactivation function (Wu et al., 2000). The A/B domain of TRα also contains a nuclear localization sequence (NLS-2) which is absent from the TRβ isoform (Mavinakere et al., 2012).

The DNA-binding domain (DBD) is most conserved across the NR superfamily (Lazar et al., 1991; Jin and Li, 2010; and Mondal et al., 2016). The DBD contains two "zinc finger" motifs and recognizes thyroid hormone response elements (TREs) (Lazar et al., 1991, Yen et al., 2001; Yen et al 2006; Mondal et al., 2016). The TRE consensus sequence (also known as a "half-site") is 5'-AGGTCA-3'. Half-sites can be arranged as direct, palindromic, or inverted palindromic repeats and may be separated by a short, random sequence of bases (Miyamoto et al., 1993; Velasco et al., 2007; Paquette et al., 2014).

The hinge domain is a flexible linker domain thought to orient the DBD and the ligand binding domain (LBD) on TREs (Pissios et al., 2000; Jin and Li, 2010). However, the hinge domain also plays a role in stabilizing TR after ligand binding or following interactions with corepressors (Pissios et al., 2000; Yen et al., 2001). Helix-1(H1) and Helix-2(H2) of the hinge

region are incorporated in the conserved LBD structure of TR (Pissios et al., 2000). While H1 and H2 do not interact directly with the ligand, they play major roles in maintaining total protein stability and stability of the ligand-binding cavity (Pissios et al., 2000; Wagner et al., 1995). The stabilization of TR seems to rely on LBD-hinge interactions, which are induced by TH when ligand-bound and by nuclear corepressor (NCoR) in the absence of TH (Pissios et al., 2000). The hinge domain also contains NLS-1 which is conserved between TRα and TRβ (Yen et al., 2001; Mavinakere et al., 2012).

The LBD is a multifunctional domain. It mediates ligand binding, ligand-dependent transactivation, and regulates coregulator interactions and dimerization (Yen et al., 2001; Mondal et al., 2016). Including H1 and H2 of the hinge domain, the conserved LBD structure contains 12 α-helices (H1-H12) which form an antiparallel "α-helix sandwich" (Jin and Lin, 2010). H12 of the LBD contains activation function-2 (AF-2), a leucine-rich sequence which facilitates ligand-dependent transactivation (Yen et al., 2001). The LBD contains at least two nuclear export signals (NES), one within H12 (NES-H12) and one (or two) spanning H3 and H6 (NES-H3/H6) (Mavinakere at al., 2012).

Intracellular Trafficking of Thyroid Hormone Receptors

Although a higher density of TR accumulates in the nuclear compartment, TR shuttles rapidly between the nucleus and cytoplasm (Bunn et al., 2001; Grespin et al., 2008; Mavinakere et al., 2012). TR relies on karyopherins—importins and exportins—for efficient nucleocytoplasmic trafficking (Bunn et al., 2001; Mavinakere et al., 2012; Submaranian et al., 2015; Roggero et al., 2016). This process requires RanGTP to facilitate cargo exchange (Figure 4).

Importins recognize basic amino acid sequences found in the NLS of the hinge or the A/B domains. TR interacts with importin 7 and importin α1/β1 (Roggero et al., 2016). Nuclear export is influenced by a calreticulin/exportin 1 (CRT/CRM1) dependent pathway and by exportins 4, 5, and 7 (XPO4, XPO5, and XPO7) (Grespin et al., 2008; Submaranian et al., 2015). While XPO5 and XPO7 directly affect nuclear export, XPO4 has an indirect effect on nucleocytoplasmic shuttling. Knockdown of XPO4 alters the rate of TR transport, but not the overall distribution (Submaranian et al., 2015).

The intracellular distribution of TR relies on protein interaction partners as well as inherent nuclear trafficking motifs. Interestingly, the DNA binding ability of TR does not affect its nuclear-to-cytoplasmic distribution. However, TRs deficient in the ability to bind their coregulator NCoR shift towards a cytosolic distribution (Yen et al., 2006). Addition of common heterodimer partner retinoid-X-receptor (RXR) induces a return to nuclear localization. This suggests that the stability conferred by nuclear binding partners—such as NCoR and RXR—may augment nuclear retention.

TR Regulation of Gene Expression

Thyroid hormone receptors bind to TREs as monomers, homodimers, or heterodimers with RXR. If unassociated with ligand, TR recruits corepressors, such as NCoR and silencing mediator for retinoid and thyroid hormone receptor (SMRT) (Cheng et al., 2010; Schoenmakers et al., 2013; Yen et al., 2016). The corepressor complex recruits histone deacetylases to induce tight packing of the DNA, blocking access by transcriptional machinery (Cheng et al., 2010; Brent, 2012; Yen et al., 2016). The interaction domains of corepressors contain an LXXXIXXXL/I motif which is recognized by TR (Yen et al., 2001; Jin and Li, 2010).

The binding of T_3 induces a conformation change in the AF-2/H12. Helix 12 encloses the ligand like a "lid," changing the surface structure of the LBD (Quack and Colberg, 2001; Jin and Li, 2010). This leads to dissociation of corepressors and recruitment of coactivators with binding motif LXXLL (Jin and Li, 2010). The corepressor and coactivator binding sites overlap; thus, the conformation change of TR in response to ligand-binding is a crucial part of inducing transactivation via coregulator exchange (Jin and Li, 2010). Coactivators of TR include steroid receptor coactivators (SRC-1, SRC-2, and SRC-3), vitamin D receptor interacting protein/TR associated protein complex (DRIP/TRAP), and CREB-binding protein (Quack and Colberg, 2001; Yin et al., 2006; Schoenmakers et al., 2013). SRC-1 recruits histone acetyltransferases to neutralize DNA-histone interactions and open DNA. DRIP/TRAP is thought to act as an anchoring protein which recruits RNA polymerase II (Yin et al., 2006).

The concentrations of TR, RXR, and T_3, the organization of half-sites, and the sequence or flanking sequence of TREs affect the prevalence of TR monomers, homodimers, or heterodimers. Monomers are sufficient to binds to TREs. TRα1 monomers are capable of binding TREs, adopting agonist conformation, and binding coactivators of TR (SRC-1, TRAP/DRIP), but are more susceptible to destabilization when changes are introduced in half-sites or flanking sequences (Quack and Colberg, 2001). Furthermore, monomers and TR/RXR heterodimers coexist in limiting RXR concentrations, signifying that the role of monomeric TR in gene expression depends on the expression levels of both binding partners (Quack and Colberg, 2001). Homodimer prevalence increases with TR concentration (Lazar et al., 1991; Miyamoto et al., 1993). Homodimerization of TR also depends on the isoform. Some studies report almost negligible TRα homodimer formation, while others detect both TRβ and TRα homodimers bound to TREs (Lazar et al., 1991; Nagaya et al., 1996; Velasco et al., 2007). TRβ homodimerizes

more readily than TRα, and at lower concentrations (Lazar et al., 1991; Miyamoto et al., 1993; Velasco et al., 2007). T_3 may also destabilize certain homodimer complexes from TREs (Miyamoto et al., 1993).

The organization of the TRE also affects the binding of TR monomers and dimers. The direction of the repeat (direct, palindromic, or inverted palindromic) and the length of the spacers between half-sites favors certain TR complexes. (Forman et al., 1992; Nagaya et al., 1996; Velasco et al., 2007; Paquette et al., 2014). Overall, TR/RXR heterodimers have more stability than monomers and homodimers and are more versatile (Lazar et al., 1991; Nagaya et al., 1996; Quack and Colberg, 2001; Wu et al., 2001; Velasco et al., 2007; Paquette 2014). Heterodimers are more tolerant of changes in consensus sequence and flanking nucleotides; they also have adequate binding affinity across all TRE types (Quack and Colberg, 2001; Velasco et al., 2007; Paquette 2014).

Role of Thyroid Hormone Signaling in Development and Disease

Thyroid hormone signaling regulates development across vertebrates. Experiments using the frog *Xenopus tropicalis* highlight the prominent, yet divergent, roles TRα and TRβ play in tadpole metamorphosis. TRβ knockouts (TRβKO) delay tail regression, as is exhibited by a decrease in mRNA expression of extracellular matrix-degrading enzymes in the tail (Nakajima et al., 2018). Olfactory nerve reduction and gill absorption are also slower in TRβKO tadpoles (Nakajima et al., 2018). TRα knockout (TRα KO), interestingly, does not halt metamorphosis; TRαKO tadpoles complete metamorphosis more rapidly, consistent with the observation that the high levels of TRα expressed throughout tadpole development repress certain metamorphosis-inducing genes (Choi et al., 2017; Schreiber 2017). TRα also affects gut remodeling. TRαKOs

had less folds in their intestinal lumen, resulting in a shorter gastrointestinal tract than their wild-type counterparts (Choi et al., 2017).

A retroviral oncogene of TRα1, v-ErbA, is carried by the avian erythroblastosis virus (AEV). v-ErbA is incapable of binding T_3 and exhibits dominant-negative effects on the function of both TRα1 and its heterodimer partner, RXR (Bonamy et al., 2005; Bondzi et al., 2011). Dominant-negative inhibition occurs due to v-ErbA introducing competition for TREs and TR coregulators (Bonamy et al., 2005). However, this oncogene also disrupts the shuttling of TRα. The expression of v-ErbA in tandem with WT-TRα lead to colocalization of both receptors in cytosolic inclusions (Bonamy et al., 2005).

Thyroid-related malfunction of the TH-signaling pathways also affects human health and development. Mutations in TR have been found in several types of cancer, including thyroid cancer, breast cancer, renal cell carcinoma, and hepatocellular carcinoma (Kim et al., 2012). Epigenetic silencing of TR also relates to cancer progression. A study of differentiated thyroid cancer found hypermethylation of the TRβ promoter and the subsequent decrease of TRβ mRNA positively correlated with cancer progression. Treatment with a demethylation agent reduced proliferation and migration (Kim et al., 2012). An analysis of 227 triple-negative breast tumors found that low TRβ expression corresponded with poor clinical outcomes in patients with triple negative breast cancer (TNBC) (Gu et al., 2015). shRNA knockdown of TRβ in TNBC-representative cell lines resulted in increased colony formation and decreased sensitivity to the chemotherapy drugs docetaxel and doxorubicin. Overexpression or stimulation with TRβ agonists reversed the poor clinical phenotype, reducing cell growth and increasing chemosensitivity. An excess or deficit of TH circulating through the body also has adverse effects on health. Symptoms of hypothyroidism are varied, but may include tiredness or lethargy,

dry skin, hair loss, shortness of breath, palpitations, and vertigo (Carle et al., 2014). Hyperthyroidism can lead to increased heart rate, osteoporosis, fatigue, muscle wasting, and damage to the eye or optic nerve (Mondal et al., 2016). Due to their impact on metabolic functions, mutations in TR or other TH-regulatory proteins, such as deiodinases, are linked to obesity and type-2 diabetes (Mondal et al., 2016).

Resistance to Thyroid Hormone Syndrome

Failure of TR to mediate TH-signaling results in Resistance to Thyroid Hormone syndrome (RTH). Patients with RTH usually have mutations in the *THRA* or *THRB* gene which decrease TR ligand-binding and/or transactivation function, although there are some cases documented where no TR mutation is identified (Tylki-Szymanska et al., 2015)

RTH manifests in two distinct clinical phenotypes—RTHα and RTHβ—depending on the affected TR isoform. Mutations in *THRB* were originally identified as contributing to the RTHβ phenotype. This phenotype is characterized by high serum levels of T_4, T_3, and TSH, which is indicative of a malfunctioning negative feedback loop due to defective TRβ in the hypothalamus, pituitary, and thyroid gland (Tylki-Szymańska et al., 2015). Persons afflicted by RTHβ also experience goiter and delayed growth and development (Ortiga-Carvalho et al., 2014).

Mutations in *THRA* causing RTHα went largely unnoticed, possibly due to the near-normal TH and TSH levels exhibited by patients (Schoenmakers et al., 2013). Only in the last decade have novel *THRA* mutations showing impaired TH-sensitivity been linked to a form of RTH. Symptoms of RTHα include delayed growth and development, chronic constipation, skeletal abnormalities, and altered basal metabolic rate and resting heart rate (Moran et al., 2013; Schoenmakers et al., 2013; Ortiga-Carvalho et al., 2014).

RTH-inducing mutants can be heterozygous and, less frequently, homozygous (Ortiga-Carvalho et al 2014). Cases of autosomal dominant inheritance have been reported and RTH can be widely inherited in families (Ortiga-Carvalho et al., 2014; Tylki-Szymańska et al., 2015; Demir et al., 2016). Often, heterozygous mutations exhibit dominant-negative inhibition of their wild-type counterparts. Dominant-negative inhibition can occur between subtypes as well, as seen in reports where mutant TRβ interfered with WT-TRα function (Yen et al., 1992). Interestingly, inserting dimerization-blocking mutations into dominant-negative mutants can eliminate dominant-negative ability, suggesting that the formation of inactive mutant-and-wild-type TR heterodimers may be a means of inhibiting wild-type TR function (Nagaya et al., 1993). Cases of RTH range from mild to severe, depending on the mutation. As sensitivity to TH varies by the case, certain patients can improve with T_4 therapy (Moran et al., 2013; Moran et al., 2017).

TRα1 Mutant A382PfsX7

A case study isolated a heterozygous, dominant-negative TRα1 mutant A382PfsX7 in a female patient with RTHα (Moran et al., 2013). The patient exhibited classic RTHα-attributed symptoms such as obesity, short stature, macrocephaly, chronic constipation, and delayed development of motor and language skills. Several features—a low free-T_4: free-T_3 ratio, subnormal rT_3 levels, and epilepsy— were less common, but linked to other RTHα phenotypes produced in mouse models.

In the RTHα patient, a guanine nucleotide deletion elicited a frameshift beginning at codon 382, and the amino acid specified by the codon changed from alanine to proline. Six subsequent residues were altered; the final substitution inserted a stop codon which truncated the receptor at codon 388 (Figure 6). This premature stop codon deleted 22 C-terminal amino acids,

including a portion of H11 and the entire H12. A382PfsX7 does bind T_3 nor does it exhibit transactivation capabilities. The removal of H12 exposed a hydrophobic cleft which facilitated constitutive corepressor binding (Moran et al., 2013).

Investigation of the Intracellular Localization of Mutant A382PfsX7

Decreased transactivation function allows mutant TRs to exert deleterious effects on development, growth, and metabolism that culminate in RTH. However, investigation into how mutations within localization signal sequences affect the disease phenotype has been sparse. Since TR function relies in part on maintaining the balance of nuclear and cytosolic TR, aberrative transport of the mutant could be tied to a molecular profile of RTHα. Altered shuttling of the mutant suggests an alteration in transcriptional activity – whether it be repressive or activating.

The truncation of A382PfsX7 eliminates H12 of the LBD, removing AF-2 and NES-H12 (Moran et al., 2013). This thesis assesses whether the elimination of the second NES in the LBD affects the intracellular localization of A382PfsX7. Since the mutation described is heterozygous, both individual expression of A382PfsX7 and WT-TRα1 and coexpression of WT and mutant were studied. Given that most RTH mutations characterized are heterozygous, evaluating the behavior of coexpressed mutant and WT has clinical relevance (Ortiga-Carvalho et al., 2014). Prior to the experiment, it was predicted that the mutant would show increased nuclear distribution relative to WT, due to the deletion of an export signal This increased nuclear localization was expected be seen in the coexpression treatment as well. Furthermore, the mutant was assayed for aggregation that may be linked to dominant-negative inhibition, as was observed in the oncoprotein v-ErbA (Bondzi et al., 2011).

EXPERIMENTAL DESIGN

Construction of Recombinant Protein mCherry-A382PfsX7 Plasmid

An A382PfsX7 expression plasmid (GeneArt) was inserted into an mCherry expression vector with a CMV promoter (Clontech) via restriction enzyme digest (Figure 7). The insert and vector contained complementary cleavage sites for KpnI and BamHI restriction endonucleases (New England Biolabs). For the initial digest, 4 µg of the plasmid, 4 µl of 10x NEBuffer, 20 units of KpnI (amounting to 2 µl), and ddH_20 to 40 µl were digested for five hours in a 37°C waterbath. Vector and insert were purified using a QIAquick PCR Purification Kit (Qiagen). The elution was then digested with 10x NEBuffer, 20 units of BamHI (amounting to 1 µl), and ddH_20 to 40 µl at 37°C for 5 hours.

Vector and insert were run in 10x glycerol-dye loading buffer on an agarose gel to separate undigested, partially digested, and fully digested fragments. Undigested mCherry and A382PfsX7 and a 2-log ladder were included in the run as references. Electrophoresis was performed for 40 minutes at a constant 100 volts. Following completion of the run, the gel was stained with ethidium bromide (1 µg/ml). Fully digested vector and insert were cut from the gel and extracted using a QIAquick Gel Extraction Kit (Qiagen). A 1:3 ratio of vector-to-insert was incubated overnight with T4 ligase and T4 10x ligase buffer at 16°C. Following its successful ligation, the mCherry-A382PfsX7 gene construct was transformed in NEB-5alpha Competent *E. coli* using New England Biolabs High Efficiency Transformation Protocol for C2987H cells. Transformed *E. coli* were amplified in LB-media containing 30 µg/ml kanamycin and grown shaking at 300 rpm, 37°C. DNA was extracted by a ZymoPURE Plasmid Midiprep (Zymo Research) and the concentration measured on a NanoDrop ND-1000 spectrophotometer (Thermo Scientific**).** Prior to use, the plasmid was sequenced (Molecular Gene Lab, Biology Department,

College of William and Mary) to confirm successful construction of an mCherry-tagged A382PfsX7 expression plasmid. Expression plasmid for wild-type human TRα1 tagged with enhanced green fluorescent protein (eGFP-hTRα1) was obtained from a glycerol stock kept by the Allison Lab. A portion of glycerol stock was grown shaking as described above in LB-media containing kanamycin. DNA extraction was performed using ZymoPURE Plasmid Midiprep and the concentration was measured using the NanoDrop ND-1000.

Cell Culture and Transfection

Work with cell lines was done in a Class II Biological Safety Cabinet. HeLa cells were maintained at 37°C in an 83 cm^3 culture flask in 20 ml of Minimal Essential Medium (MEM)(Gibco) with 10% Fetal Bovine Serum (FBS) containing a phenol red pH indicator. When cell confluency became 80%, cells were split to a lower density in a new flask.

Identical procedures for the localization assay and the aggregation assay were used, with the only difference being the method of scoring. Experimental trials were performed in 6-well plates (Figure 7). Twenty-four hours before the intended transfection, HeLa cells were seeded at ~ 2.5×10^5 cells per well with 2 ml of MEM (+10%FBS). Cells were incubated at 37°C for a day, or until confluency was ~70%. Each well was transfected with 2 μg of plasmid (2 μl), 4 μl of Lipofectamine 2000, 494 μl Opti-MEM, and 1.5 ml of MEM (+10% FBS) for a total volume of 2 ml. Plates were incubated for 8 hours and then the media was replaced with 2 ml of MEM (+10% FBS). Twenty-four hours after the start of the transfection, the plate was removed from the incubator, fixed with 3.7% formaldehyde solution (9.6 ml ddH2O, 1.2 ml 37% formaldehyde, and 1.2 ml 10x D-PBS), stained with a drop of FluoroMount + DAPI, and placed upon slides. Three treatments were applied across each transfection: (1) eGFP-hTRα1, (2) mCherry-A382PfsX7, and (3) eGFP-hTRα1 + mCherry-A382PfsX7. Individual WT and mutant

transfections utilized 2 μg of the respective plasmid. Cotransfections used 2 μg DNA total with 1 μg each of WT and mutant plasmid. The complete transfection of a 6-well plate was considered one independent replicate. The experiment was replicated four times.

Localization Assay Scoring and Analysis

Slides were assessed using a Nikon Eclipse TE2000-E inverted microscope (Nikon) and NIS-Elements AR 3.2. Oversaturated regions were identified and adjusted accordingly for scoring.100 cells were scored per slide, amounting to 800 cells scored per treatment across the four replicates. The intracellular distribution of the recombinant proteins was indicated by calculating the average nuclear-to-cytoplasmic (N:C) ratio of fluorescence intensity across treatments. Regions of interest (ROIs) were selected in both the nucleus (RIO_1) and cytoplasm (ROI_2). ROIs were placed in areas with even TR distribution and the placement of ROIs on aggregates was avoided to prevent over-or-underestimations of the N:C ratio. The ROI intensity was collected and exported from NIS-Elements into Excel for analysis. Each scored cell was evaluated at the two ROIs, and two measurements of the nuclear and cytoplasmic intensity were exported. For cells scored in the coexpression treatment, intensity of both WT and mutant were reported separately. The mean N:C ratio of each slide was calculated. Data were exported to R version 3.3.2 for statistical analysis. Results were analyzed with an unpaired, two-tailed Student's *t*-test. The significance level was set at $\alpha = 0.05$ for all analyses. The normality of the data collected was verified by a Shapiro-Wilk test for normality and generation of a quantile-quantile plot prior to computation of the *t*-test statistic.

Aggregation Assay Scoring and Analysis

The presence of aggregation was assessed qualitatively. Cells were scored for the presence or absence of aggregates. Four replicates were conducted, and 100 cells were scored per

slide. One slide of the cotransfection treatment was eliminated due to improper placement of the coverslip. Data were analyzed in R version 3.3.2. The frequency of aggregates was analyzed using a Pearson's chi-square test for independence with a significance level $\alpha = 0.05$. The successive pairwise comparisons were done using a chi-square test for independence. To account for the increased rate of type I error, a Bonferroni Correction was applied to the significance level, reducing it to $\alpha = 0.01\overline{6}$. The chi-square analysis of the 2 x 2 contingency included a Yates continuity correction. The magnitude of effect between treatments was calculated with an odds ratio

RESULTS

Coexpression of WT-TRα1 and A382PfsX7 Increases Cytosolic Distribution

Limited response to T_3 and deficiencies in transactivation are well-documented molecular characteristics of nonfunctional, RTH-inducing TR mutants (Moran et al., 2013; Ortiga-Carvalho et al., 2014; Moran et al., 2017). Constitutive corepressor binding has also been implicated (Moran et al., 2013; Schoenmakers et al., 2013). Conducive to these observations, RTH mutations commonly manifest in the LBD, which regulates these functions. Less studied is whether certain LBD mutations may also affect TR trafficking. Mutations causing RTH may overlap with NES regions in the LBD, suggesting that some cases of RTH may showcase altered TR shuttling. Analysis of oncoprotein v-ErbA indicates that aberrant intracellular localization may be another hallmark of dominant-negative inhibition (Bonamy et al., 2005). While TRα primarily localizes to the nucleus, v-ErbA expression induces a shift of TRα and heterodimer partner RXR to the cytoplasm. Mislocalization of TR may affect its function as a transcription factor.

To determine whether the nonfunctional TRα1 mutant A382PfsX7 mislocalized due to the deletion of its second NES, eGFP-hTRα1 and mCherry-A382PfsX7 were expressed, individually and concurrently, in HeLa cells. HeLa cells express negligible endogenous TR (Selmi and Samuels, 1991); thus, the only TR acting in the cell would be that which was introduced artificially. Although WT-TR may passively diffuse into the nucleus, the TRs used in this experiment were tagged with fluorescent proteins. These recombinant proteins were too large to diffuse through nuclear pore complexes, ensuring that (1) any nucleocytoplasmic trafficking that occurred would be mediated by importins/exportins and (2) TR would require functional NLS/ NES to interact with these transporter proteins.

Despite the loss of NES-H12, the mutant A382PfsX7 did not display a significant shift in nuclear-to-cytoplasmic distribution when compared to WT-TRα1 (Figure 8; $p = 0.1922$). Unexpectedly, the cotransfection of WT and mutant produced a subtle cytosolic shift in TR distribution. The cotransfected WT and cotransfected mutant had a significantly lower N:C ratio compared to their individually transfected counterparts (Figure 9; *coexpressed-WT vs WT*: $p = 0.0007$*; Figure 10; *coexpressed-A382PfsX7 vs A382PfsX7*: $p = 0.0001$*). However, it may be noted that while the N:C ratio decreased slightly, yet significantly, the overall distribution of both mutant and WT remained predominantly nuclear (Figure 11). These results were contrary to the initial prediction that deletion of an NES would increase mutant presence in the nucleus. It was concluded that the A382PfsX7 mutation alone did not alter intracellular distribution. Instead, the results suggest that a novel interaction between A382PfsX7 and WT-TRα1 may occur that is sufficient to either sequester TR in the cytoplasm or decrease retention in the nucleus.

Table 1: Localization of A382PfsX7 and WT-TRα1				
Treatment	$\bar{x}_1$	$\bar{x}_2$	T-statistic	P-value
A382PfsX7 vs. WT	2.458	2.551	-1.3702	0.1922
Cotransfected WT vs. WT	2.204	2.551	-4.2915	**0.0007***
Cotransfected A382PfsX7 vs. A382PfsX7	2.177	2.458	-5.2384	**0.0001***

Co-transfection of WT-TRα1 and A382PfsX7 Shows Increased Presence of TR Aggregates

Aggregation could be a potential explanation for shifts in intracellular distribution. Previous characterization of the TRα1 oncoprotein v-ErbA by the Allison lab determined that it alters nucleocytoplasmic transport, shifting the typical nuclear distribution of TR towards the cytosol (Bonamy et al., 2005; Bonamy and Allison, 2006). Furthermore, v-ErbA accumulates in cytosolic foci which display hallmarks of the aggresome—a highly regulated compartment facilitating proteasome-mediated degradation of misfolded proteins—formation (Bondzi et al., 2011).

Aggregation occurs when nonpolar amino-acid residues are exposed to the aqueous intracellular environment and self-associate into β-structures (Silva et al., 2013; De Baets et al., 2015). Aggregation prone regions (APRs) are usually buried in the hydrophobic core of proteins, where they can be stabilized by tertiary interactions. Residues that comprise APRs have high hydrophobicity and low net charge. Gatekeeper residues that surround most APRs prevent aggregation (De Baets et al., 2015). These residues tend to be enriched with acidic or basic (glutamate, aspartate, lysine, arginine), large and flexible (lysine or arginine), or β-structure-incompatible (proline or glycine) amino acids (De Baets et al., 2015). Mutations or damage to

either the APR, the gatekeeper residues, or adjacent tertiary stabilizing residues could all increase the aggregation potential of a polypeptide.

Aberrant aggregation of functional and nonfunctional proteins is potentially another means of the dominant-negative inhibition displayed by many TR mutants and may contribute to the dysregulation of TH-target genes. Aggregation could also affect the mislocalization of shuttling proteins. The removal of H12 due to the A382PfsX7 mutation increases access to the hydrophobic cleft accommodating corepressors. Furthermore, the deletion of 22 C-terminal amino acids suggests residues they once stabilized are available to form novel interactions, potentially with their aqueous environment. To determine whether RTH-inducive mutant A382PfsX7 displayed aberrant TR aggregation, HeLa cells transfected with the receptor(s) of interest were analyzed for aggregate formation after the 24-hour incubation. The subcellular location of aggregates present was recorded; however, due to the subjectivity of the former assessment, only the explicit presence or absence of aggregates was analyzed statistically.

The initial 3x2 test for association between treatment and aggregation was significant (Chi-square test, P-value $< 2.2 \times 10^{-16}$). Treatments were further assessed by pairwise comparisons. The frequency of aggregates in cells expressing either WT or mutant differed significantly from that of the coexpression treatment (*WT vs. Cotransfection*: P-value $< 2.2 \times 10^{-16}$; *A382PfsX7 vs. Cotransfection*: P-value $< 2.2 \times 10^{-16}$). In a majority of cells scored, colocalization between A382PfsX7 and WT-TRα1 was observed within aggregates (Figure 12). However, colocalization was not assessed quantitatively. The differing magnitudes of aggregation were assessed by an odds ratio. The odds of success ("success" defined as the presence of TR aggregates) in the cotransfection treatment was 2.665 and 3.507 times higher than the odds of success within WT and A382PfsX7 treatments respectively. As a reference, the

odds ratio between the WT and A382PfsX7 was calculated ($\widehat{OR}$= 1.315). The results show that a significant increase in aggregation occurs under co-expression of WT and A382PfsX7, further supporting the notion that a novel interaction occurs between mutant and WT-TR.

Table 2: Comparison of TR Aggregation Across Treatments

Comparison	Chi-Square Test Statistic	P-value
WT vs. A382PfsX7 vs. Cotransfection	142.26	**< 2.2 x 10^-16***
WT vs. A382PfsX7	5.1962	0.02645
WT. vs Cotransfection	79.168	**< 2.2 x 10^-16***
A382PfsX7 vs. Cotransfection	121.51	**< 2.2 x 10^-16***

Table 3: Magnitude of Aggregation

Comparison	Odds Ratio	Upper 95% Confidence Interval	Lower 95% Confidence Interval
Cotransfection vs. WT	2.665	3.317	2.142
Cotransfection vs. A382PfsX7	3.507	4.405	2.791
WT vs. A382PfsX7	1.315	1.666	1.039

DISCUSSION

Localization and the Dominant-Negative Effect of A382PfsX7

Contrary to expectations, the lack of NES-H12 in A382PfsX7 had no effect on its intracellular distribution, suggesting that this mutant is capable of shuttling between the nucleus and cytoplasm with an efficacy similar to WT. It may be that NES-H3/H6 in the LBD or the CRM1/calreticulin dependent NES (location unknown) are sufficient to maintain normal nuclear export in the absence of NES-H12. Interestingly, the coexpression of A382PfsX7 and WT produced a small, but statistically significant shift of TR distribution towards the cytosol. It is worth noting that the TR distribution within co-transfected cells remained predominantly nuclear. Yet, it does suggest that heterozygous RTH-inducing mutations may affect the cellular phenotype differently than homozygous mutations, perhaps due to the dominant-negative inhibition exhibited by many TR mutants. However, since such inhibition also occurs between subtypes, homozygous mutations do not necessarily preclude the potential for dominant-negative effects between TRα and TRβ, which were not tested for in this thesis. In lieu of its altered subcellular distribution when co-expressed with WT, A382PfsX7 was analyzed for its ability to promote aggregation of TR. The frequency of aggregation between individually transfected WT and A382PfsX7 did not differ significantly from expected values. However, HeLa cells co-expressing WT and A382PfsX7 did show a significant increase in TR aggregates. The odds ratio of co-transfected cells showcasing aggregation was increased 2-3 times that of the individual transfections

That the mutation alone was insufficient to alter subcellular distribution and aggregation implies a novel protein-protein interaction between WT and A382PfsX7 that affects TR localization when the two are coexpressed. There is evidence that interactions between WT

and mutant TR affect both localization and aggregate formation, as seen in the dominant-negative oncoprotein v-ErbA, which shifts WT-TRαl distribution towards the cytosol and displays colocalization with WT in cytosolic aggregates (Bonamy et al., 2005; Bondzi et al., 2011). Altered subcellular localization and aggregation of TR following coexpression of WT-TRα1 and A382PfsX7 may be related to the dominant-negative inhibitory effect displayed by certain heterozygous RTH mutants. Dominant-negative inhibition has several theorized mechanisms. Most commonly postulated are (1) mutant or nonfunctional WT/mutant heterodimers competing for TRE binding sites or (2) titration out of RXR or other TR auxiliary factors due to association with TR mutants (Matsushita et al., 2000; Bonamy et al., 2005; Bonamy and Allison, 2006; Bondzi et al., 2011). Dominant-negative inhibition of TR function implies that a mutant disrupts WT function in the nucleus. Mutant TR may directly impede WT function by obstructing access to TREs or auxiliary factors. Alternatively, skewing the nuclear-to-cytoplasmic distribution of WT-TR, as is shown here, indirectly affects TR transcriptional regulation by limiting the amount of WT capable of interacting with TH-target genes. Furthermore, since TRs are capable of repression and activation of genes without TH-interaction, a skew in TR distribution could affect gene expression regardless of the direction of the shift.

Investigating heterozygous RTH-causing variants with mutations in the import or export sequences may elucidate whether mislocalization is linked to disease pathogenesis or dominant-negative inhibition. However, that WT localization showed a significant deviation from the norm only when coexpressed with A382PfsX7 implies protein-protein interactions influence the latter's dominant-negative inhibition of WT and that the altered N:C distribution may stem from this interaction. Protein-protein interactions are commonly associated with dominant-negative ability. An RTH-inducing TRβ mutant, L428R, which has impaired

dimerization function, displays no dominant-negative inhibition of WT (Matsushita et al., 2000). This is further supported by the finding that restoring the ninth heptad of the TR dimerization sequence to natural TR-inhibitor TRα2—a C-terminal variant with little T_3 or RXR affinity—augments its dominant-negative effect (Burgos-Trinidad and Koenig, 1999). This supports that the TR dimerization motif—a series of heptad repeats in the LBD— plays a key role in regulating whether mutants exhibit dominant-negative function. The dimerization region spans residues 279 to 372, which contains H11 of the LBD (Selmi and Samuels 1991). In addition to the deletion of H12, the A382PfsX7 frameshift alters six residues within H11 before the premature C-terminal deletion. This may elicit abnormal dimerization of A382PfsX7 due to destabilization of H11 and may be responsible for the unusual localization seen in the coexpression of WT and mutant.

WT/A382PfsX7 Coexpression and Aggregate Formation

The A382PfsX7 frameshift changes the amino acid residues at codons 382 through 388 from Ala-Ser-Arg-Phe-Leu-His-Met to Pro-Ala-Ala-Ser-Ser-Thr-STOP. Aggregation prone regions tend to be enriched with hydrophobic or aromatic amino acids such as valine, phenylalanine, tyrosine, and isoleucine (Prabakaran et al., 2017). A382PfsX7 does not gain many hydrophobic residues due to the frameshift. A majority of the changes result in amino acids that are less characteristic of APRs. Serine and threonine, both hydrophilic amino acids, and proline, whose ring structure is incompatible with β-sheet secondary structures, are reduced in APRs and less likely to form the β-strand interactions necessary for aggregation (De Baets et al., 2015; Parbakaran et al., 2017). Proline is also a known gatekeeper residue that prevents APRs from aggregating (De Baets et al., 2015; Prabakaran et al., 2017). The change in primary protein structure, as caused by the A382PfsX7 mutation, does not appear to increase aggregation

propensity of the receptor. It seems more likely that the deletion of H12 exposes hydrophobic side chains, which previously had been shielded by the α-helix, to the surrounding solvent. The receptor may alter shape to accommodate the new interactions between hydrophobic side-chains and the aqueous cell environment, increasing its potential for self-assembly into β-sheets.

Aggregated proteins are not involved in nucleocytoplasmic trafficking and could contribute in part to the altered N:C ratio of the coexpressed TR. The increased cytosolic presence of TR could be due to premature sequestration in the cytoplasm or decreased retention in the nucleus. To that regard, further investigation into the intracellular mobility of A382PfsX7 would be beneficial. A study found that DNA-binding is not required for the nuclear retention of TRβ, but knockdown of NCoR shifts TRβ distribution to the cytosol (Yen et al., 1992). Addition of RXR precipitated an increase in nuclear TR density (Yen et al., 2006). This suggests that forming a stable complex within the nucleus enhances nuclear retention as auxiliary factors—such as NCoR and RXR—may compete with exportins for TR-binding. That A382PfsX7 has functional DNA-binding and an increased proclivity for its corepressors implies that A382PfsX7 can form stable nuclear complexes. Thus, the altered N:C ratio in the co-expression treatment may more likely be the result of premature cytosolic sequestration.

Formation of WT-mutant heterodimers also may play a role in the aggregation of A382PfsX7 with WT-TRα1. Compared to TRβ, TRα is less prone to homodimerization (Miyamoto et al., 1993). However, WT-mutant TRα1 heterodimers may be more stable than their respective homodimers. The alterations to A382PfsX7 structure may increase the aggregation propensity of the heterodimer, trapping mutant and WT-TRα1 in cytosolic inclusions. However, observing the aggregation of RTH mutants may be more relevant under physiological conditions where TH-signaling occurs. T_3 stimulation can disassociate homodimers from TREs and favors

TR/RXR heterodimers (Hao et al., 1994; Miyamoto et al., 1993). T_3 exposure was able to partially reverse TRα shift to cytosol in v-ErbA and WT co-expression in mouse cells, decreasing the strong correlation between TRα1 and v-ErbA colocalization (Bonamy et al., 2005). Cells exposed to physiological levels of thyroid hormone may be less likely to form protein aggregates due to preferential TR-RXR interaction, and thus show less colocalization of WT and mutant in aggregates. If T_3 affects aggregation, the affected peripheral tissues of a patient may showcase less aggregation than the cell line tested here, although perhaps more so in cases of RTHβ where TH levels are constitutively high.

Alternatively, misfolded TR mutants may lead to a prion-like induction of the misfolding and sequestration WT. More recently, some pathogenic mutations have been found to induce prion-like misfolding of their WT counterparts. The R248Q mutant of tumor suppressor gene p53 is shown to act as a “seed” which facilitates aggregation of WT-p53, p63, and p73 (Ano Bom et al., 2012). This “seeding” ability is a hallmark of prion (protein misfolding) diseases. Furthermore, aggregating cancerous p53 mutants are theorized to act in a dominant-negative manner wherein one mutant in a p53 tetramer is sufficient to cause loss-of-function and lead to prion-like sequestration of WT p53 (Silva et al., 2013). However, if A382PfsX7 does induce prion-like misfolding and accumulation, it is unusual that the singular expression of A382PfsX7 did not show a significant increase in aggregation. If A382PfsX7 increased the mutant’s intrinsic aggregation propensity, it would be expected to aggregate regardless of WT presence. This suggests that the interaction between WT and A382PfsX7 increases the aggregation potential of both receptors, rather than A382PfsX7 being a prion-like inducer of aggregation.

Implications of Aggregation on RTH Therapeutic Practices

Disease mutations causing aggregation require cells to devote more energy to protein quality control to ensure proper refolding or degradation of misfolded proteins. Molecular chaperones and heat shock proteins must be recruited to refold or stabilize misfolded proteins. Otherwise, misfolded protein aggregates and must be targeted for destruction via (1) ubiquitin-tagged proteasome degradation, (2) lysosomal-mediated removal, or (3) aggresome recruitment for proteasome degradation (Bondzi et al., 2011). Analysis of the aggregates precipitated by v-ErbA show they colocalize with aggresomal markers GFP-250 and GFP-170 (Bondzi et al., 2011). In this study, it was noted that the most common location of WT/A382PfsX7 aggregates was perinuclear (Figure 12; data not shown). This suggests travel to the perinuclear microtubule organizing center, which is a hallmark of aggresome formation (Bondzi et al., 2011). It is unknown whether aggregation and aggresome formation is cytoprotective or a result of the pathogenesis of disease mutants. However, in support of the cytoprotective potential of aggregate formation, downregulation of aggregation-promoting interface acetyltransferase p300 correlates with increased toxicity in cancerous p53 mutants due to debilitated proteasome activity (Silvia et al., 2013).

Protein aggregation is being more frequently recognized as a factor in human diseases, even outside of traditional protein-misfolding diseases such as Alzheimer's disease, Parkinson's disease, and prion diseases (Silvia et al., 2013). A comprehensive analysis of the human proteome found that mutations which increase the intrinsic aggregation potential of a protein are more significantly associated with pathogenic mutants than neutral mutants (Da Baets et al., 2015). Since aggregation affects a protein's function, trafficking, and degradation, any associated pathways could be potential therapeutic targets in aggregation-inducing diseases.

Furthermore, the subcellular characteristics of a pathogenic mutant could indicate the severity of a disease or the response to a therapeutic approach. For example, there is a correlation between p53 aggregation and tumor aggressiveness (Silva et al., 2013). The presence of α-galactosidase aggregates in cases of Fabry disease (a lysosomal storage disorder) can be used to predict patients' responsiveness of DGJ[1] therapy with 77.5 percent accuracy (Siekierska et al., 2012). T_4 therapy is a common treatment in thyroid-responsiveness disorders. Mutant TRs in RTH display reduced or negligible TH-binding, but less severe mutations can increase transactivation and reverse dominant-negative inhibition when exposed to higher levels of T_3 (Chatterjee et al., 1991). In less severe cases of RTH, T_4 therapy can increase the growth rate and improve the body composition of the patient (Moran et al., 2017). It can also be used to normalize basal metabolism (Moran et al., 2013). Aggregation of WT and mutant TR could affect the outcome of T_4 therapy on the clinical phenotype of RTH, due to its limiting of functional TR able to respond to the TH signal. Gauging a mutant's aggregation potential could be a useful indicator of a person's response to T_4 therapy.

[1] DGJ: 1-deoxygalactonojirimycin

REFERENCES

Ano Bom, A., Rangel, L., Costa, D., de Oliveira, G., Sanches, D., Braga, C., Gava, L., Ramos, C., Cepeda, A., Stumbo, A., De Moura Gallo, C., Cordeiro, Y., Silva, J. (2012). Mutant p53 Aggregates into Prion-like Amyloid Oligomers and Fibrils. Journal of Biological Chemistry, 287(33): 28152-28162.

Bonamy, G. and Allison, L. (2006). Oncogenic Conversion of the Thyroid Hormone Receptor by Altered Nuclear Transport. Nuclear Receptor Signaling, 4:1-5.

Bonamy, G., Guiochon-Mantel, A., and Allison, L. (2005). Cancer Promoted by the Oncoprotein v-ErbA May Be Due to Subcellular Mislocalization of Nuclear Receptors. Molecular Endocrinology, 19(5): 1213-1230.

Bondzi, C., Brunner, A., Munyikwa, M., Connor, C., Simmons, A., Stephens, S., Belt, P., Roggero, V., Mavinakere, M., Hinton, S., and Allison, L. (2011). Recruitment of the Oncoprotein v-ErbA to Aggresomes. Molecular and Cellular Endocrinolgy, 332:196-212.

Brent, Gregory. (2012). Mechanisms of Thyroid Hormone Action. The Journal of Clinical Investigation, 122(6): 3035-3043

Bunn, C., Neidig, J., Freidinger, K., Stankiewicz, T., Weaver, B., McGrew, J., and Allison, L. (2001). Nucleocytoplasmic Shuttling of the Thyroid Hormone Receptor α. Molecular Endocrinology, 15(4):512-533.

Burgos-Trinidad, M., and Koenig, R. (1999). Dominant Negative Activity of Thyroid Hormone Receptor Variant a2 and Interaction with Nuclear Corepressors. Molecular and Cellular Endocrinology, 149: 107-114.

Carle, A., Bulow-Pedersen, I., Knudsen, N., Perrild, H., Ovesen, L., and Laurberg, P. (2014). Hypothyroid Symptoms and the Likelihood of Overt Thyroid Failure: A Population-Based Case-Control Study. European Journal of Endocrinology, 171(5): 93-602.

Chatterjee, V., Nagaya, T., Madison, L., Datta, S., Rentoumis, A., and Jameson, J. (1991) Thyroid Hormone Resistance Syndrome: Inhibition of Normal Receptor Function by Mutant Thyroid Hormone Receptors. J. Clin. Invest., 87: 1977-1984.

Cheng, S., Leonard, J., and Davis, P.J. (2010). Molecular Aspects of Thyroid Hormone Actions. The Endocrine Society, 31(2): 139-170.

Choi, J., Ishizuya-Oka, A., and Buchholz, D. (2017) Growth, Development, and Intestinal Remodeling Occurs in the Absence of Thyroid Hormone Receptor α in Tadpoles of Xenopus tropicalis. Endocrinology 158(6): 1623-1633.

De Baets, G., Van Doorn, L., Rousseau, F., and Schymkowitz, J. (2015). Increased Aggregation is More Frequently Associated to Human Disease-Associated Mutations Than to Neutral Polymorphisms. Computational Biology, 11(9):1-14

Demir, K., van Gucht, A., Muyukinan, M., Catli, G., Ayhan, Y, Bas, V., Dundar, B., Ozkan, B., Meima, M., Visser, W., Peeters, R., and Visser, T. (2016). Diverse Genotypes and Phenotypes of Three Novel Thyroid Hormone Receptor-α Mutations. J Clin Endocrinol Metab, 101(8): 2945-2954.

Forman, B.M., Casanova, J., Raaka, B.M., Ghysdael, J., and Samuels, H.H. (1992) Half-Site Spacing and Orientation Determines Whether Thyroid Hormone and Retinoic Acid Receptors and related Factors Bind to DNA-Response Elements as Monomers, Homodimers, or Heterodimers. Molecular Endocrinology, 6(3):429-441.

Grespin, M., Bonamy, G., Roggero, V., Cameron, N., Adam, L., Atchison, A., Fratto, V., and Allison, L. (2008). Thyroid Hormone Receptor α1 Follows a Cooperative CRM1/Calreticulin-mediated Nuclear Export Pathway. Journal of Biological Chemistry, 283(37):25576-25588.

Gu, G., Gelsomino, L., Covington, K., Beyer, A., Wang, J., Rechoum, Y., Huffman, K., Carstens, R., Ando, S., and Fuqua, S. (2015). Targeting Thyroid Hormone Receptor Beta in Triple Negative Breast Cancer. Breast Cancer Res. Treat., 150(3): 535-545.

Halestrap, Andrew. (2012). The Monocarboxylate Transporter Family—Structure and Functional Characterization. IUBMB Life, 64(1) 1-9.

Hao, E., Menke, J., Smith, A., Jones, C., Gerrner, M., Hershman, J. Wuerth, J., Samuels,H., Ways, D., and Usala,S. (1994). Divergent Dimerization Properties of Mutant β1 Thyroid Hormone Receptors are Associated with Different Dominant Negative Activities. Molecular Endocrinology, 8(7): 841-851.

Jin, L and Li, Y. (2010). Structural and Functional Insights into Nuclear Receptor Signaling. Advanced Drug Delivery Reviews, 62:1218-1226.

Kim, W., Zhu, X., Kim, D., Zhang, L., Kebebew, E., and Cheng, S. (2013). Reactivation of the Silenced Thyroid Hormone Receptor β Gene Expression Delays Thyroid Tumor Progression. Endocrinology, 154(1): 25-35.

Lazar, M.A., Berrodin, T.J., and Harding, H.P. (1991). Differential DNA Binding by Monomeric, Homodimeric, and Potentially Heterodimeric Forms of the Thyroid Hormone Receptor. Molecular and Cellular Biology, 11(10):5005-5015.

Liu, R., Suzuki, S., Miyamoto, T., Takeka, T., Ozata, M., and DeGroot, L. (1995). The Dominant Negative Effect of Thyroid Hormone Receptor Splicing Variant α2 Does Not Require Binding to a Thyroid Response Element. Molecular Endocrinology, 9(1): 86-95.

Matsushita A., Misawa, H., Andoh, S., Natsume, H., Nishiyama, K., Sasaki, S., and Nakamura, H. (2000). Very Strong Correlation Between Dominant Negative Activities of Mutant Thyroid Hormone Receptors and Their Binding Avidity for Corepressor SMRT. Journal of Endocrinology, 167:493-503.

Mavinakere, M., Powers, J., Subramanian, K., Roggero, V., and Allison, L. (2012). Multiple Novel Signals Mediate Thyroid Hormone Receptor Nuclear Import and Export. Journal of Biological Chemistry, 287(37):31280-31297.

Miyamoto, T., Suzuki, S., and DeGroot, L. (1993). High Affinity and Specificity of Dimeric Binding of Thyroid Hormone Receptors to DNA and their Ligand Dependent Dissociation. Molecular Endocrinology, 7(2): 224-231.

Mondal, S., Raja, K., Schweizer, U., and Mugesh., G. (2016). Chemistry and Biology in the Biosynthesis and Action of Thyroid Hormones. Angewandte International Chemie, 55:7606-7630

Moran, C., Agostini, M., McGowan, A., Schoenmakers, E., Fairall, L., Lyons, G., Rajanayagam, O., Watson, L, Offiah, A., Barton, J., Price, S., Schwabe, J., and Chatterjee, K. (2017). Contrasting Phenotypes in Resistance to Thyroid Hormone Alpha Correlate with Divergent Properties of Thyroid Hormone Receptor α1 Mutant Proteins. Thyroid, 27(7): 973-982.

Moran, C., Schoenmakers, N., Agostini, M., Schoenmakers, E., Offiah, A. Kydd, A., Kahaly, G., Mohr-Kahaly, S., Rajanayagam, O., Lyons, G., Wareham, N., Halsall, D., Dattani, M., Hughes, S., Gurnell, M., Park, S., and Chatterjee, K. (2013). An Adult Female with Resistance to Thyroid Hormone Mediated by Defective Thyroid Hormone Receptor α. J Clin Endocrinol Metab, 98(11): 4254-4261.

Nagaya Takashi and J.L. Jameson. (1993). Thyroid Hormone Receptor Dimerization is Required for Dominant Negative Inhibition by Mutations that Cause Thyroid Hormone Resistance. Journal of Biological Chemistry, 268(21): 15766-15771.

Nagaya,T., Nomura, Y., Fujieda, M., and Seo, H. (1996). Heterodimerization Preferences of Thyroid Hormone Receptor α Isoforms. Biochemical and Biophysical Research Communications, 226:426-430.

Nakajima, K., Tazawa, I., and Yaoita, Y. (2018). Thyroid Hormone Receptor α- and β- Knockout Xenopus tropicalis Tadpoles Reveal Subtype-Specific Roles During Development. Endocrinology, 159(2): 733-743.

Ortiga-Carvalho, T., Sidhaye, A., and Wondisford, F. (2014). Thyroid Hormone Receptors and Resistance to Thyroid Hormone Disorders. Nat. Rev. Endocrinol., 10(10):582-591.

Paquette, M.A., Atlas, E., Wade, M.G., and Yauk, C.L. (2014). Thyroid Hormone Response Element Half-Site Organization and Its Effect on Thyroid Hormone Mediated Transcription. PLOS ONE, 9(6):1-6.

Pissios, P., Tzameli, I., Kushner, P and Moore, D.D. (2000). Dynamic Stabilization of Nuclear Receptor Ligand Binding Domains by Hormone or Corepressor Binding. Molecular Cell, 6:245-253.

Prabakaran R., Goel, D., Kumar, S., and Gromiha, M. (2017). Aggregation Prone Regions in Human Proteome: Insights from Large-Scale Data Analyses. Proteins 85: 1099-1118.

Quack, M. and Colberg, C. (2001). Single Thyroid Hormone Receptor Monomers are Competent for Coactivator-mediated Transactivation. Biochem. J., 360:387-393.

Roggero, V., Zhang, J., Parente, L., Doshi, Y., Dziedzic, R., McGregor, E., Varjabedian, A., Schad, S., Bondzi, C., and Allison. L. (2016). Nuclear Import of the Thyroid Hormone receptor α1 is Mediated by Importin 7, Importin β1, and Adaptor Importin α1. Molecular Cellular Endocrinology, 419:185-197.

Schoenmakers, N., Moran, C., Peeters, R., Visser, T., Gurnell, M., and Chatterjee, K. (2013). Resistance to Thyroid Hormone Mediated by Defective Thyroid Hormone Receptor Alpha. Biochimica et Biophysica Acta, 1830: 4004-4008.

Schreiber, Alexander. (2017). Unliganded TRα: A "Safety Lock" to Metamorphosis. Endocrine Society, 158(6) 1577-1580.

Selmi, S and Samuels, H. (1991). Thyroid Hormone Receptor/and v-erbA: A Single Amino Acid Difference in the C-terminal Region Influences Dominant Negative Activity and Receptor Dimer Formation. Journal of Biological Chemistry, 266(18): 11589-11593.

Siekierska, A., De Baets, G., Reumers, J., Gallardo, R., Rudyak, S., Broersen, K., Couceiro, J., Van Durme, J., Schymkowitz, J., and Rousseau, F. (2012). α-Galactosidase Aggregation is a Determinant of Pharmacological Chaperone Efficacy on Fabry Disease Mutants. Journal of Biological Chemistry, 287(34): 28386-28397.

Silva, J., Rangel, L., Costa, D., Cordeiro, Y, and De Moura Gallo, C. (2013). Expanding the Prion Concept to Cancer Biology: Dominant-Negative Effect of Aggregates of Mutant p53 Tumor Suppressor. Biosci. Rep. 33(4):593-603.

Subramanian, K., Dziedzic, R., Nelson, H., Stern, M., Roggero, V., Bondzi, C., and Allison, L. (2015). Multiple Exportins Influence Thyroid Hormone Receptor Localization. Molecular and Cellular Endocrinology, 411:86-96.

Tylki-Szymanska, A., Acuna-Hidalgo, R., Krajewska-Walasek, M., Lecka-Ambroziak, A., Steehouwer, M., Gilissen, C., Brunner, H., Jurecka, A., Rozdzynska-Swiatkowska, A., Hoichsen, A., and Chrzanowska, K. (2015). Thyroid Hormone Resistance Syndrome Due to Mutations in the Thyroid Hormone Receptor α Gene (*THRA*). J Med Gene, 52: 312-316.

Velasco, L., Togashi, M., Walfish, P., Passanha, R., Moura, F., Barra, G., Nguuyen, P., Rebong, R., Yuan, C., Simeoni, L., Ribeiro, R., Baxter, J., Webb, P., and Neves, F. (2007). Thyroid Hormone Response Element Organization Dictates the Composition of Active Response. Journal of Biological Chemistry, 282(17):12458-12466.

Wagner, R.L., Apriletti, J.W., McGrath, M.E., West, B.L., Baxter, J.D., and Fletterick, R.J. (1995). A Structural Role for Hormone in the Thyroid Hormone Receptor. Nature, 378: 690-697.

Wu, Y., Xu, B., and Koenig, R. (2000). Thyroid Hormone Response Element Sequence and the Recruitment of Retinoid X Receptors for Thyroid Hormone Responsiveness. Journal of Biological Chemistry, 276(6): 3929-3936.

Yen, P., Ando, S., Feng, X., Liu, Y., Maruvada, P., and Xia, X. (2006). Thyroid Hormone Action at the Cellular, Genomic, and Target Gene Levels. Molecular and Cellular Endocrinology, 246:121-127.

Yen, P., Sugawara, A., and Chin, W. (1992). New Insights on the Mechanism(s) of the Dominant Negative Effect on Mutant Thyroid Hormone Receptor in Generalized Resistance to Thyroid Hormone. Journal of Clinical Investigation, 90:1825-1831.

Yen, Paul. (2001). Physiological and Molecular Basis of Thyroid Hormone Action. The American Physiological Society, 81:1097-1142.

Figure 1: Hypothalamic-Pituitary-Thyroid Axis
A cascade of hormone signals from hypothalamus to pituitary gland to thyroid gland stimulates the production and secretion of thyroid hormone (TH). Elevated circulating free TH suppress production of thyrotropin-releasing hormone (TRH) and thyroid-stimulating hormone (TSH).

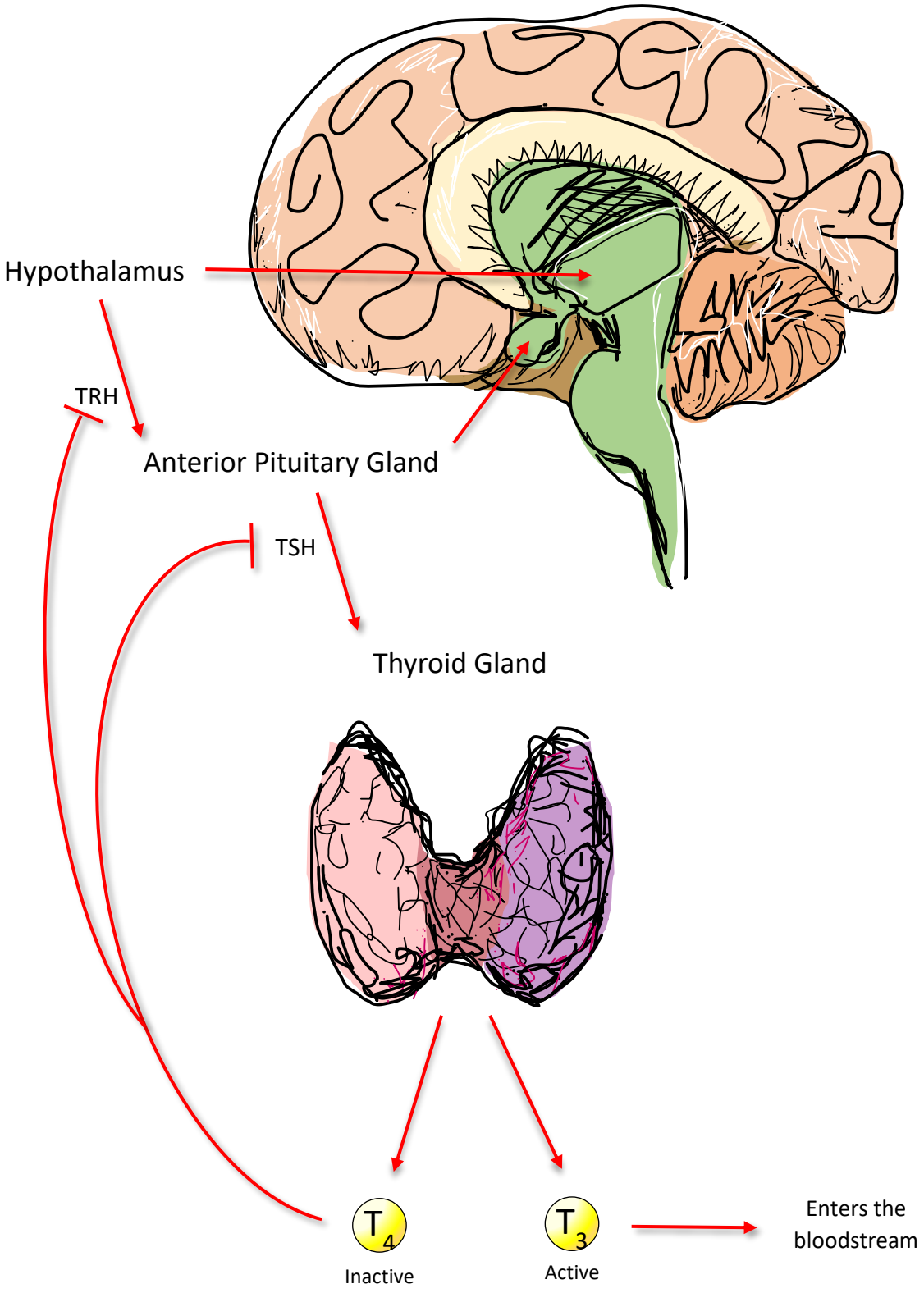

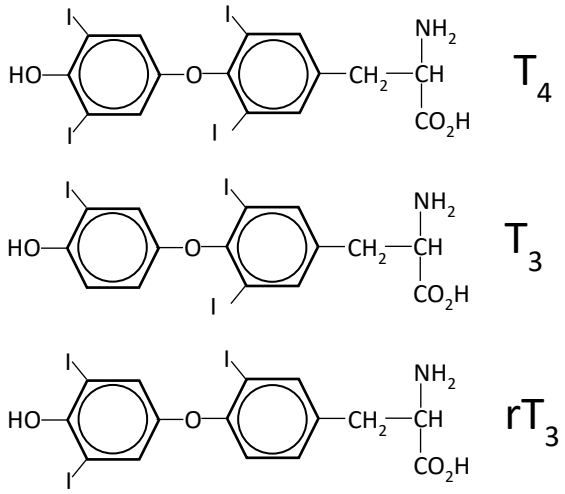

Figure 2: Forms of Thyroid Hormone
Deiodinases catalyze the removal iodide from the outer or inner carbon rings of T_4 to form active T_3 or inactive reverse T_3 (rT_3) respectively.

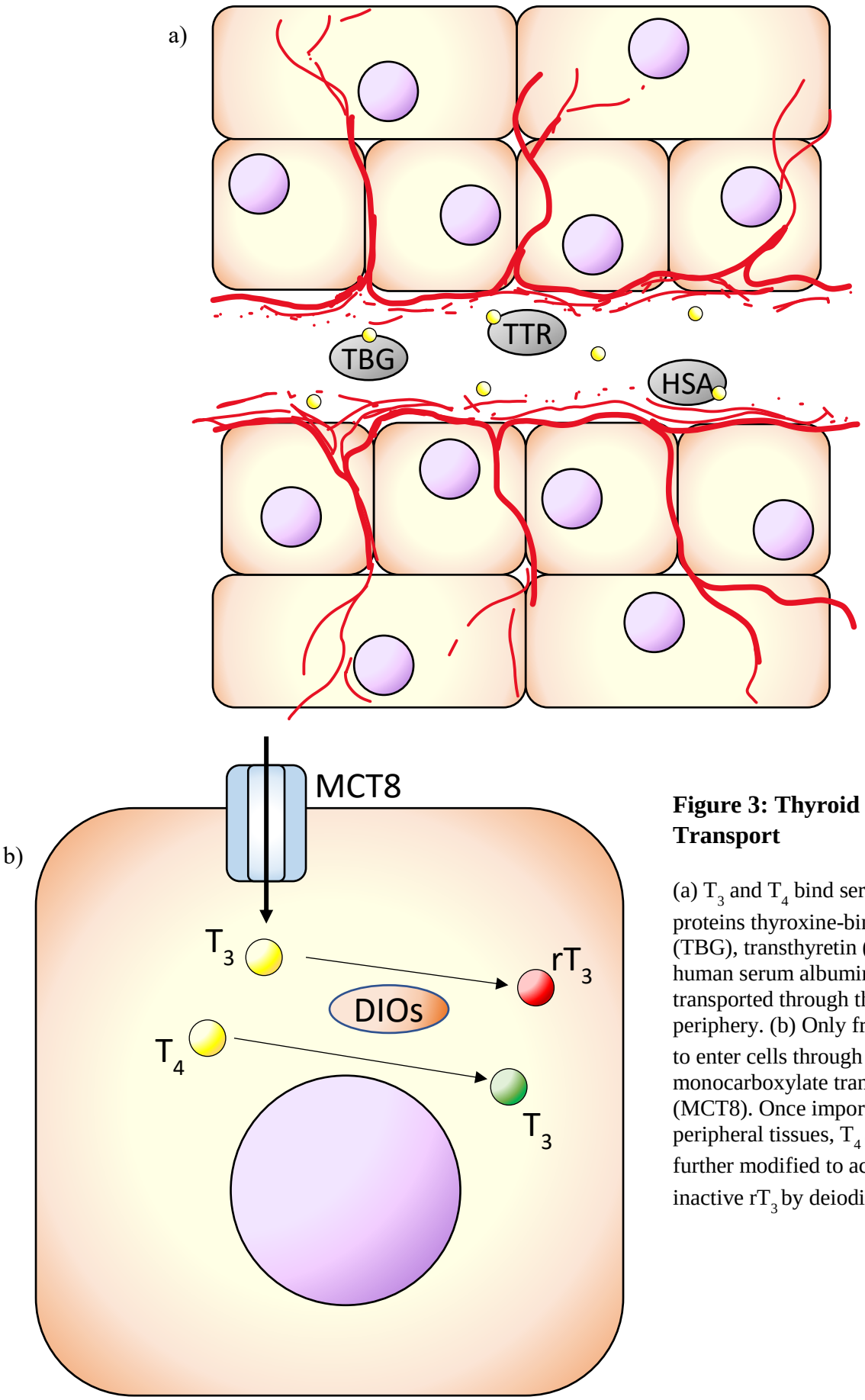

Figure 3: Thyroid Hormone Transport

(a) T_3 and T_4 bind serum transport proteins thyroxine-binding globulin (TBG), transthyretin (TTR) and human serum albumin (HSA) to be transported through the blood into the periphery. (b) Only free T_3/T_4 is able to enter cells through monocarboxylate transporter 8 (MCT8). Once imported into peripheral tissues, T_4 and T_3 can be further modified to active T_3 or inactive rT_3 by deiodinases (DIOs).

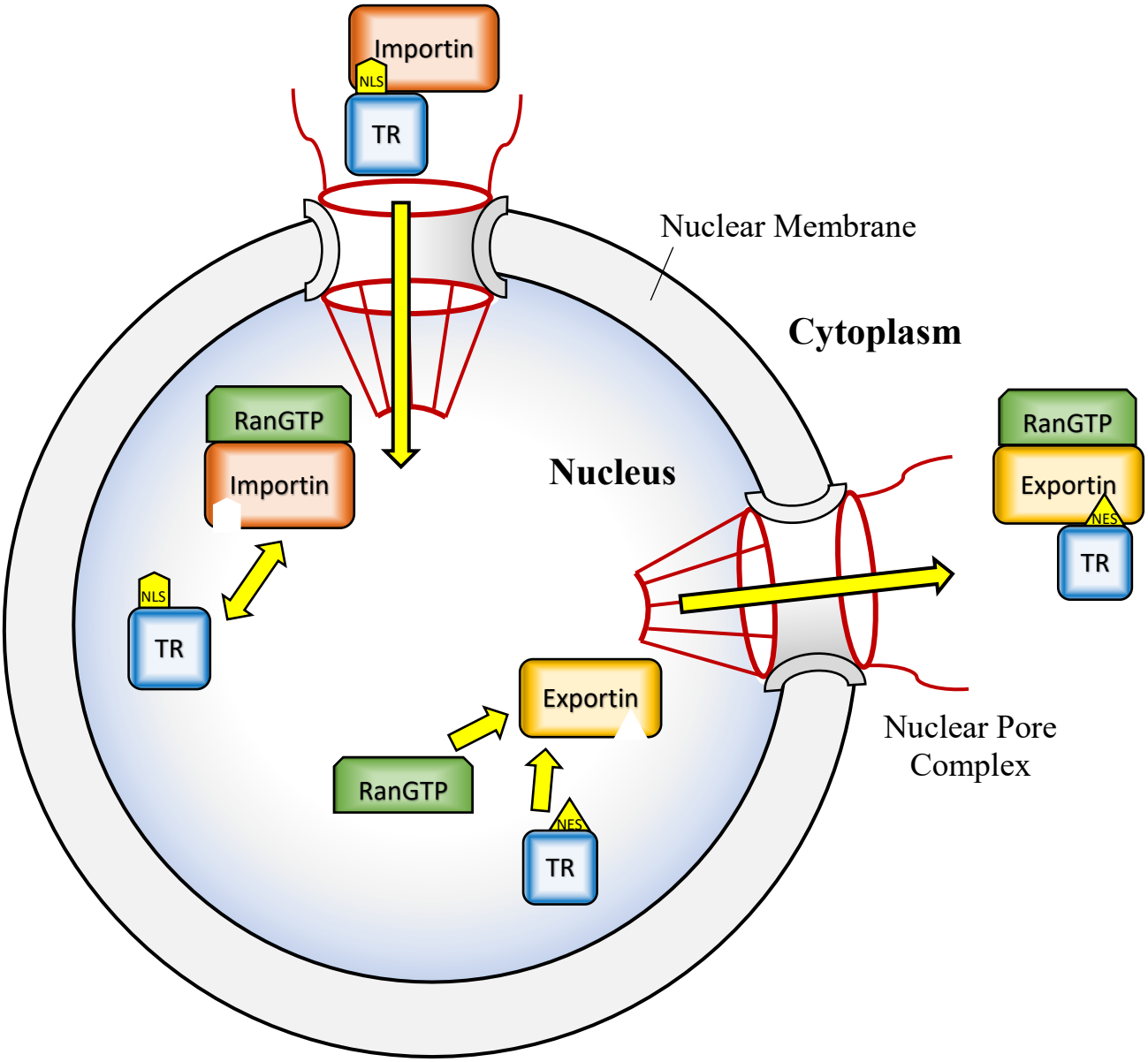

Figure 4: Thyroid Hormone Receptor Nucleocytoplasmic Transport

An importin recognizes and binds a nuclear localization signal (NLS) on TR and enables its transport across the nuclear membrane through a nuclear pore complex (NPC). Inside the nucleus, the importin binds RanGTP and undergoes a conformational change, releasing TR. Free TR disperses into the nucleus and can bind DNA. The TR nuclear export signal (NES) is bound by an exportin in conjunction with RanGTP. The TR-exportin-RanGTP complex exits the nucleus through the NPC. Once in the cytosol, RanGTP is hydrolyzed to RanGDP and the complex disassociates.

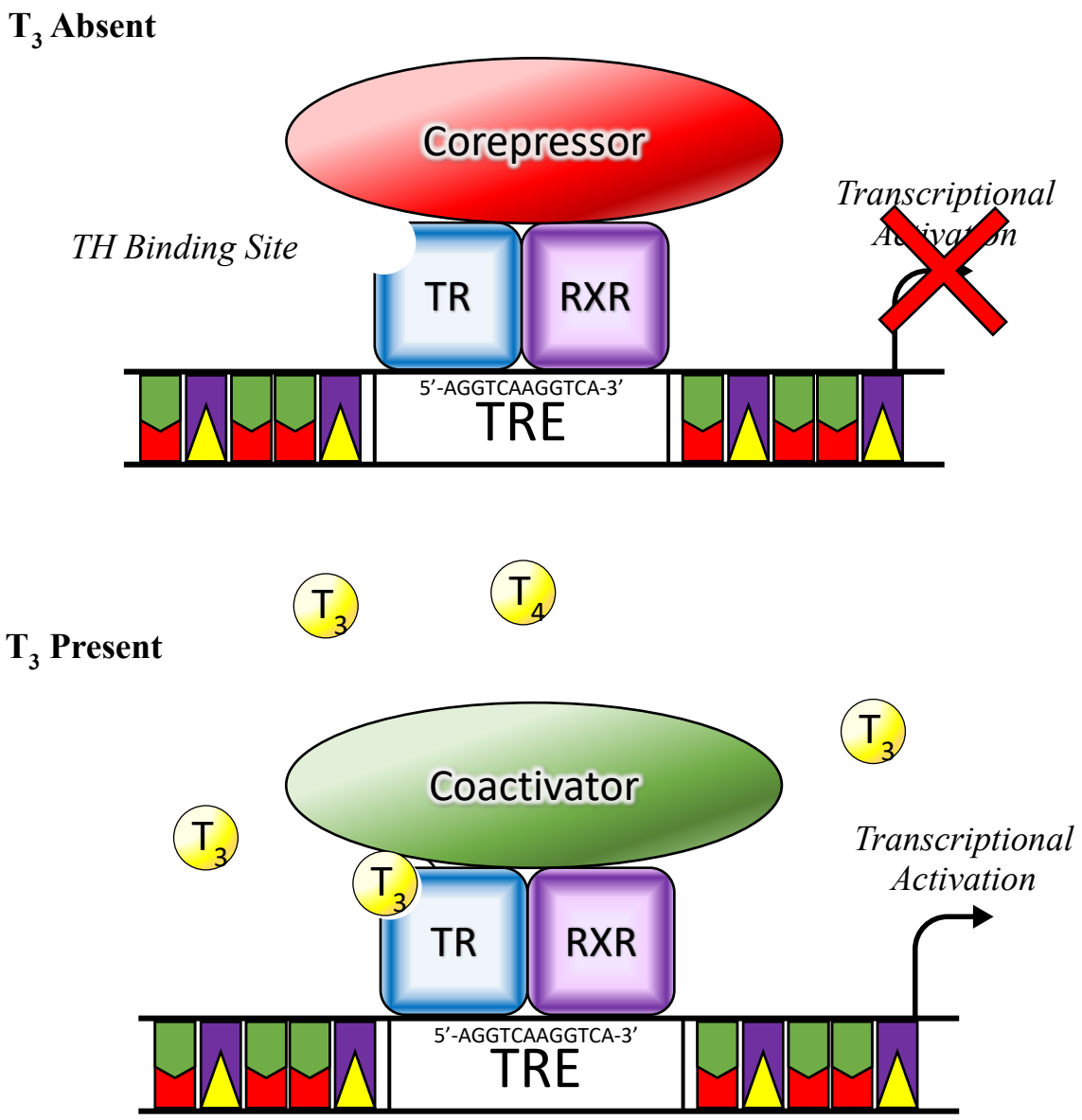

Figure 5: Regulation of Thyroid Hormone Receptor at Response Elements

(a) TR binds preferentially to TREs as heterodimers with RXR. When ligand is absent, the heterodimer binds corepressors (SMRT, NCoR) and recruits histone deacetylases to condense chromatin and limit transactivation. (b) Binding of T_3 changes the conformation of TR, leading it to recruit coactivators (SRC, DRIP/TRAP), facilitate the binding of basal transcriptional machinery, and activate transcription of the target gene.

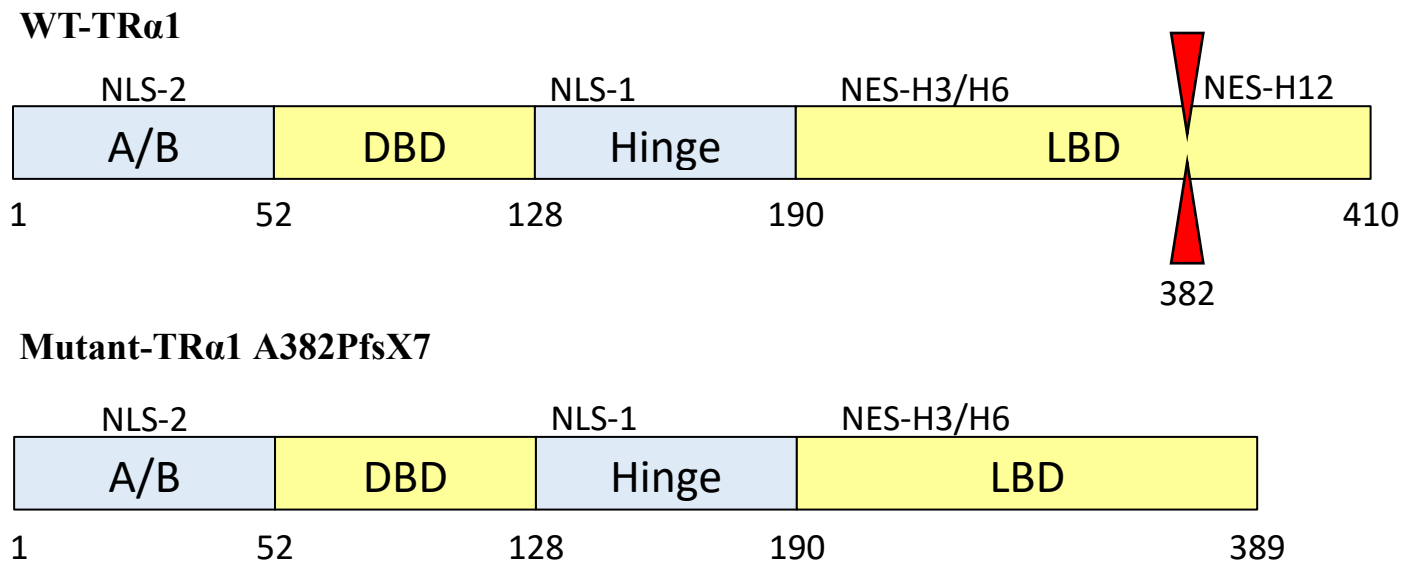

Location of Key Sequences
NLS-1: 130-147
NLS-2: 22-29
NES-H3/H6: 209-265
NES-H12: 390-407

Figure 6: Domains of TRα1 and A382PfsX7

The A382PfsX7 mutation removes 22-carboxy-terminal amino acids. Helix-12, which plays a role in nuclear export and facilitates T_3-binding is absent from the mutant structure.

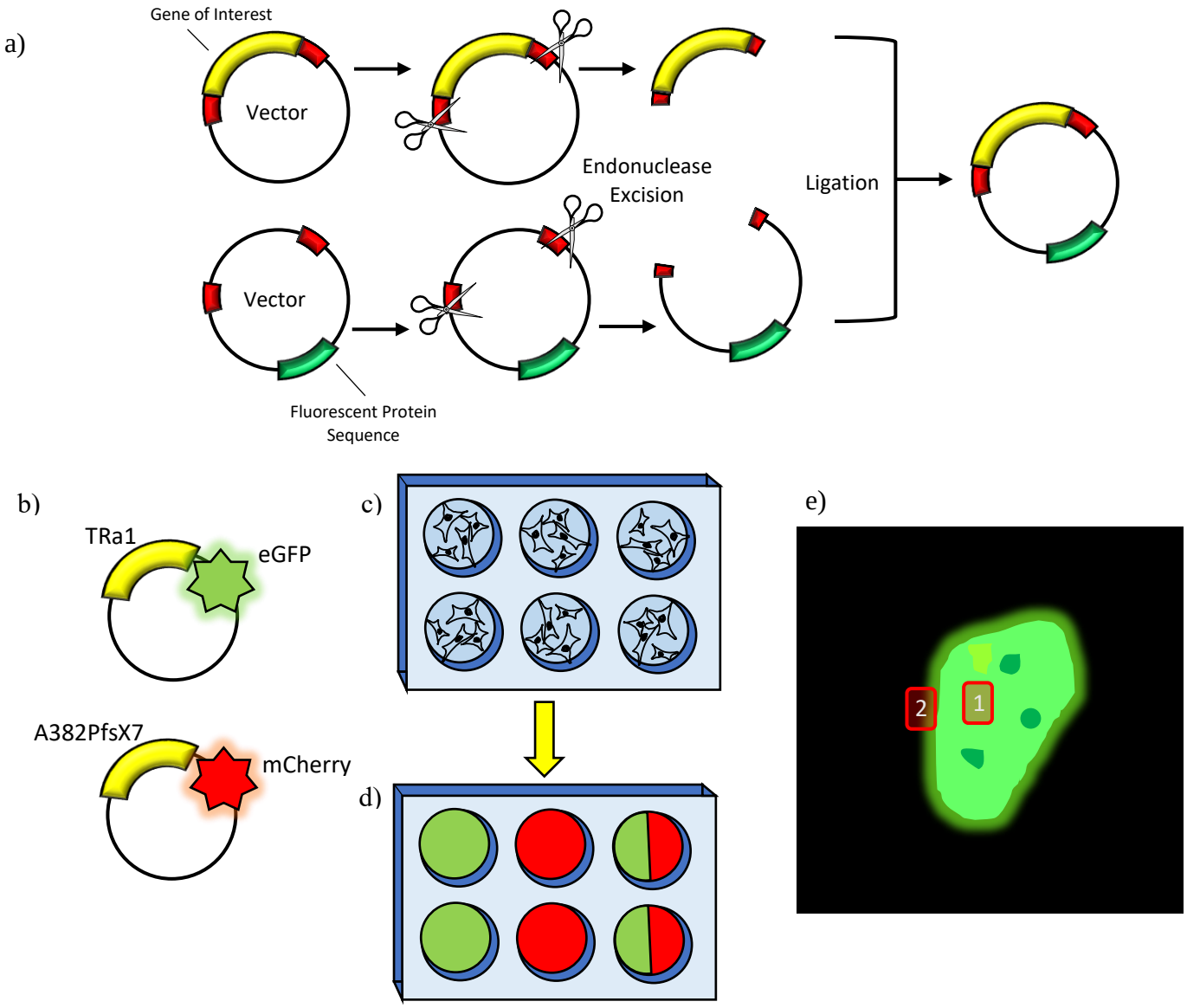

Figure 7: Experimental Methodology

(a) Gene of interest and fluorescent vector are cleaved at identical restriction sites. Complementary ends are ligated together. (b) WT TRα1 and mutant A382PfsX7 were expressed in vectors containing an eGFP and mCherry tag respectively. (c) HeLa cells were seeded at 2.5 x 10^5. (d) After a 24-hour incubation, cells were treated with the eGFP-WT plasmid (2µg), the mCherry-mutant plasmid (2µg), or both the WT and mutant plasmids (1µg each). Cells were grown for 8 hours before media change. Twenty-four hours after the start of the transfection, the cells were fixed and stained with DAPI for visualization by fluorescent microscopy. (e) Regions of interest were selected within and directly adjacent to the nucleus of cells expressing eGFP or mCherry.

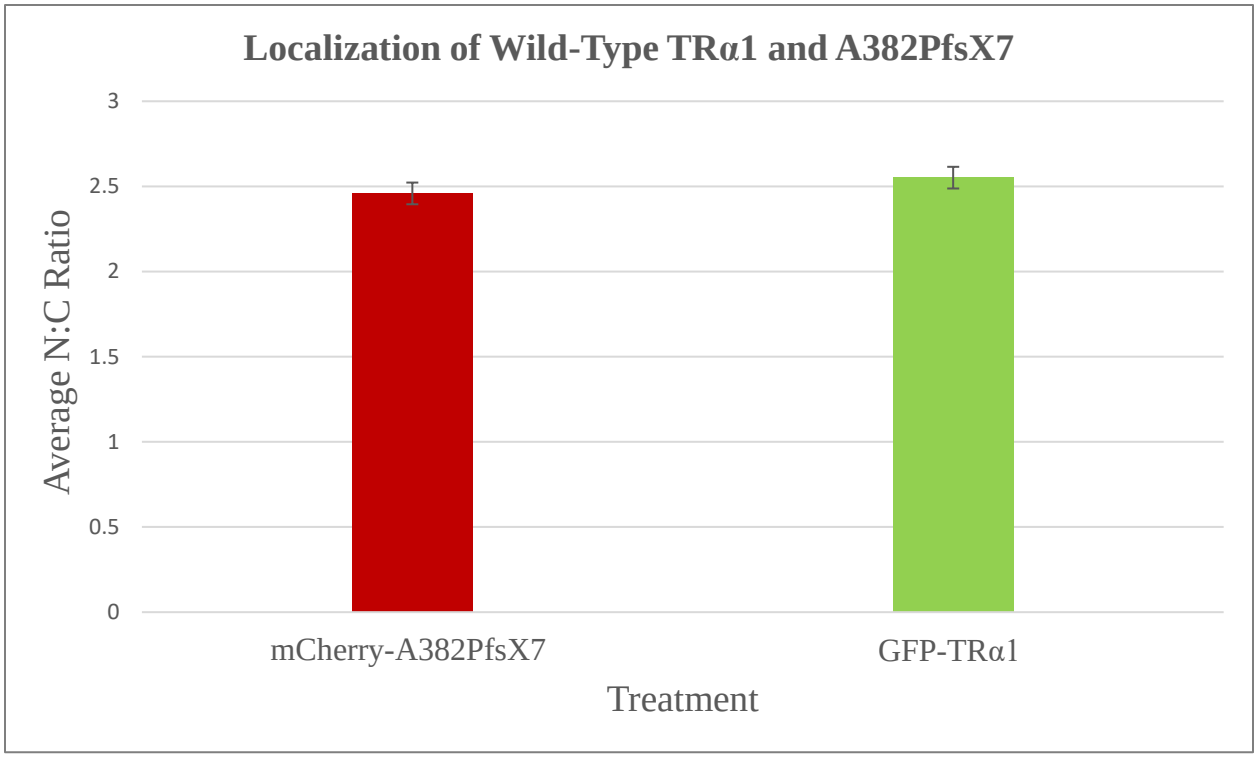

Figure 8: Localization of WT-TRα1 and A382PfsX7

No significant difference between the N:C ratio of A382PfsX7 and WT-TRα1 was observed; $p = 0.1992$; four independent replicates were tested; 600 cells scored per replicate (100 per well); bars represent mean N:C ratio of treatment indicated; error bars indicate the mean $\pm$ standard error of the difference of means

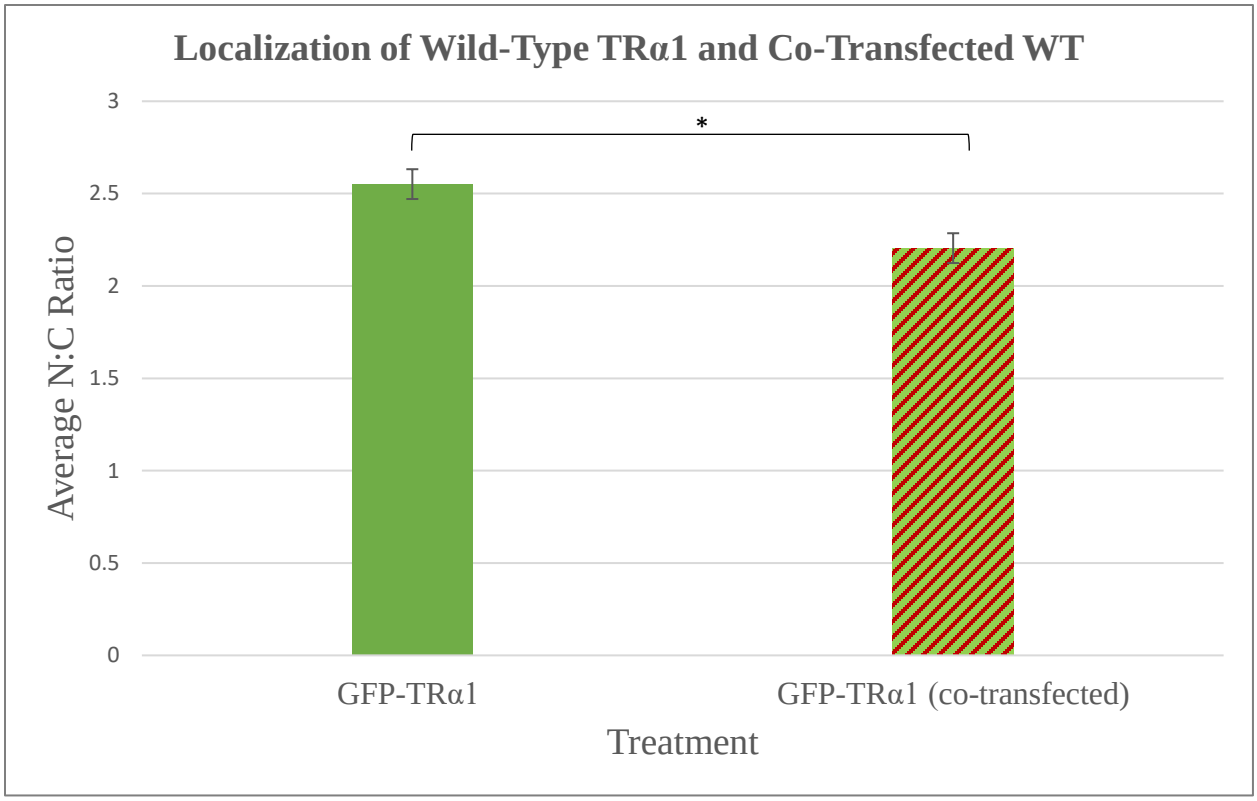

Figure 9: Localization of WT-TRα1 and Co-Transfected WT

A significant difference between the N:C ratio of WT-TRα1 and WT-TRα1 coexpressed with A382PfsXx7 was observed; $p = 0.0007$; four independent replicates were tested; 600 cells scored per replicate (100 per well); bars represent mean N:C ratio of treatment indicated; error bars indicate the mean ± standard error of the difference of means

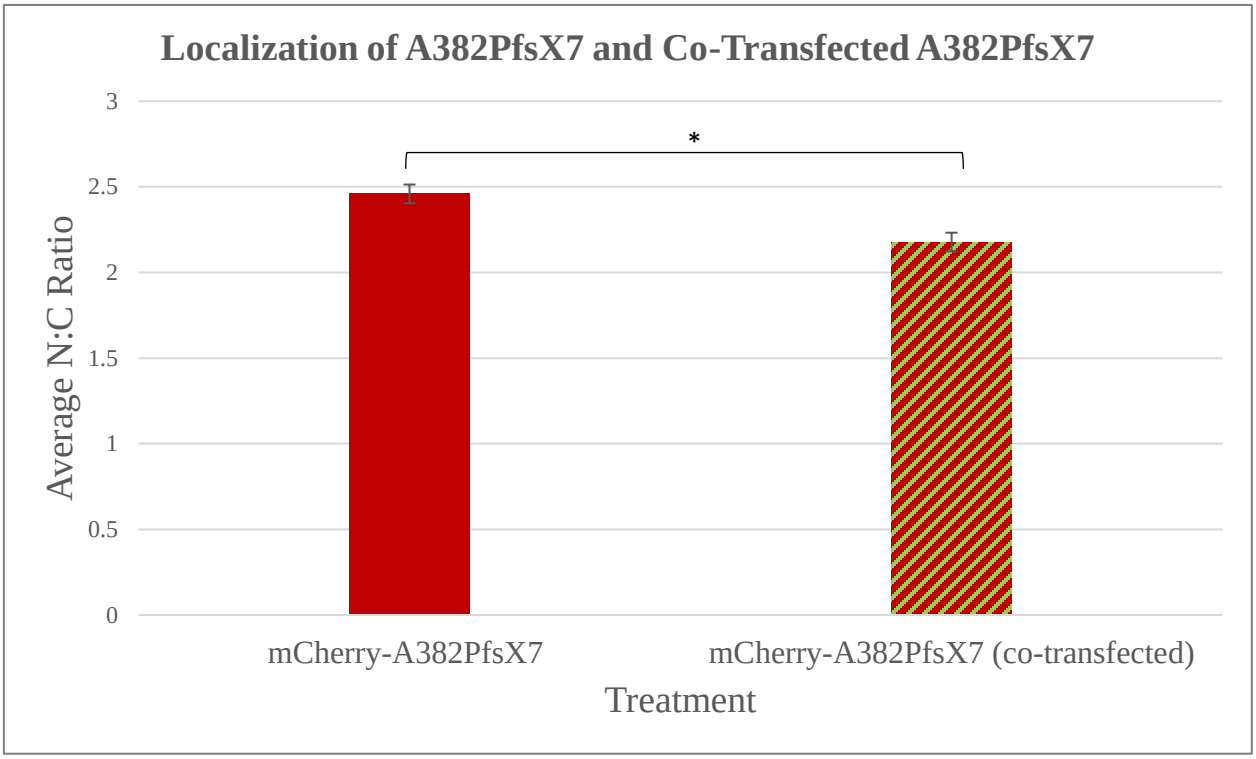

Figure 10: Localization of A382PfsX7 and Co-Transfected A382PfsX7

A significant difference between the N:C ratio of A382PfsX7 and A382PfsX7 coexpressed with WT-TRα1was observed; p = 0.0001; four independent replicates were tested; 600 cells scored per replicate (100 per well); bars represent mean N:C ratio of treatment indicated; error bars indicate the mean ± standard error of the difference of means

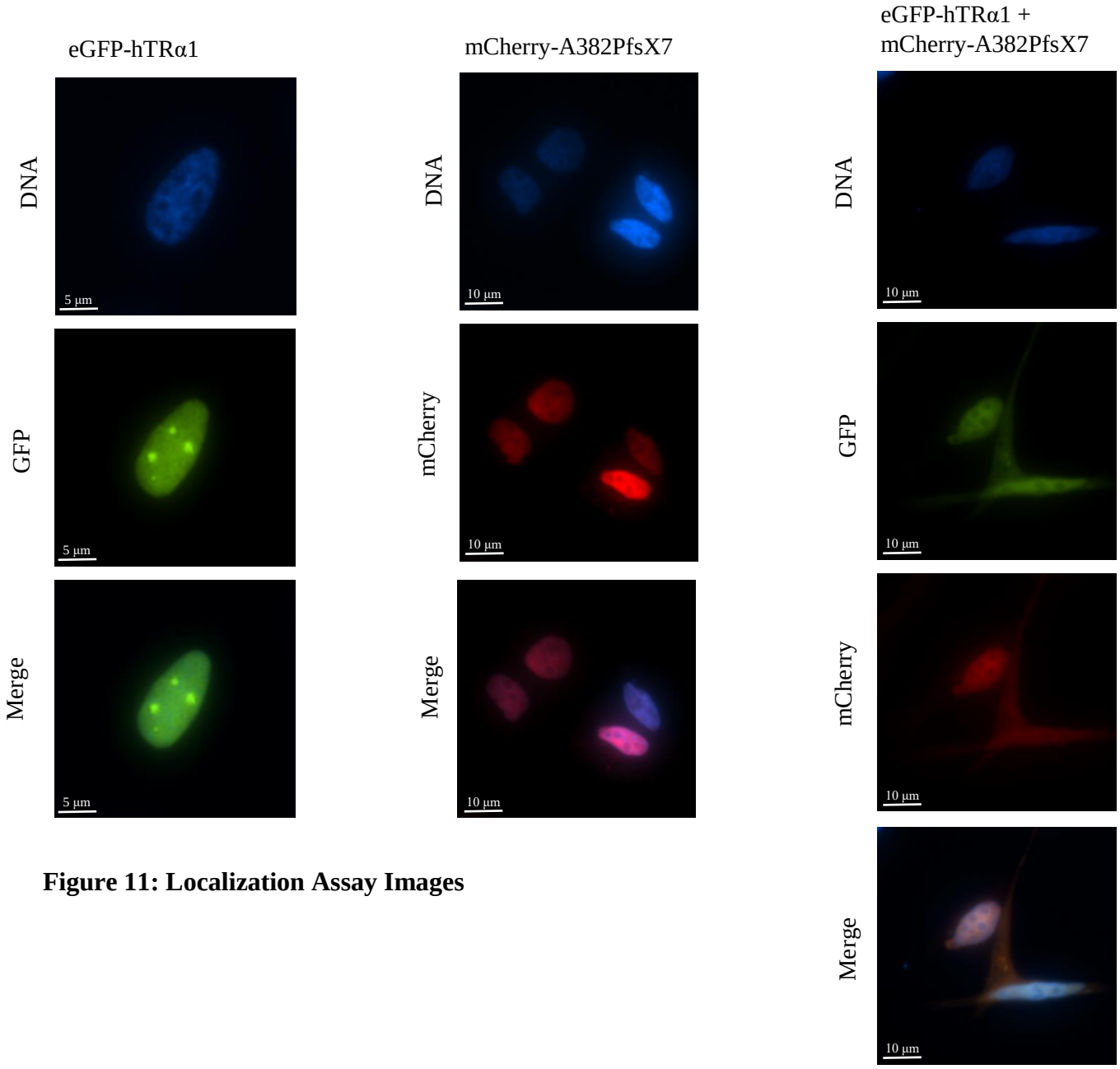

Figure 11: Localization Assay Images

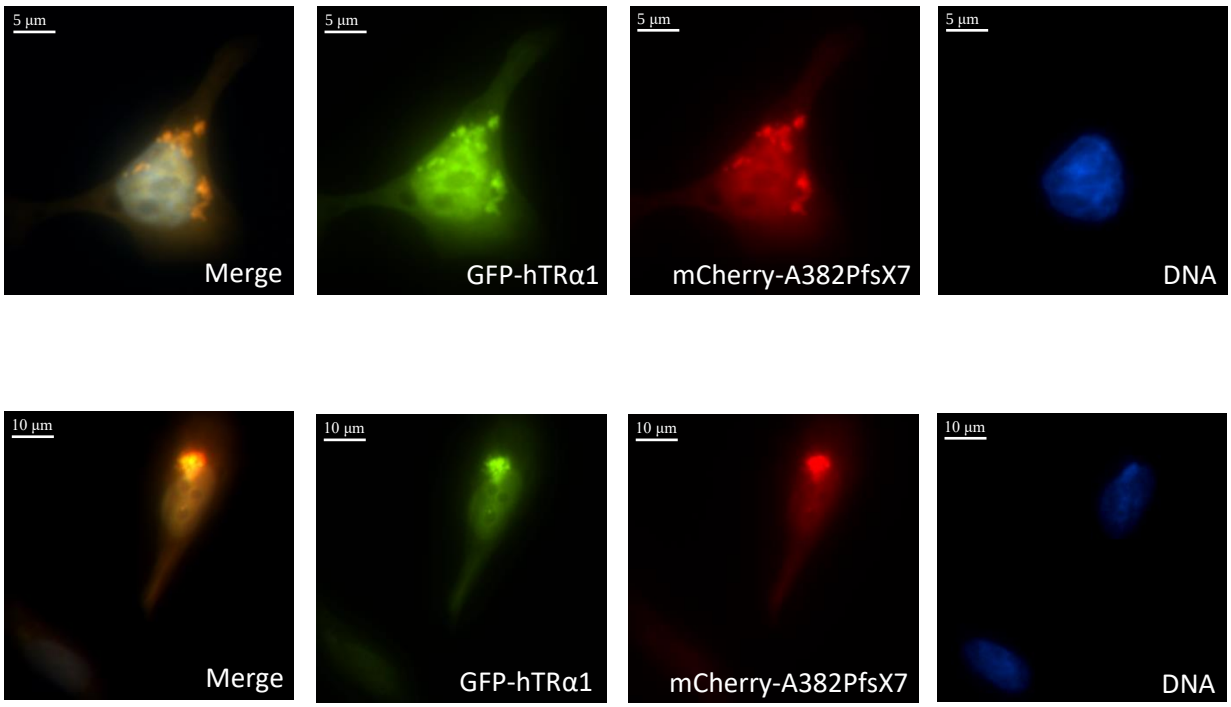

Figure 12: Presence of A382PfsX7 and WT-TRa1 Aggregates in Co-Transfected HeLa cells

Table 4: N:C Ratio Data	
Treatment	**N:C Ratio**
A382PfsX7	2.516797
A382PfsX7	2.500417
A382PfsX7	2.579932
A382PfsX7	2.395339
A382PfsX7	2.406804
A382PfsX7	2.424793
A382PfsX7	2.526203
A382PfsX7	2.362033
hTRa1	2.75242
hTRa1	2.645164
hTRa1	2.610994
hTRa1	2.404656
hTRa1	2.583635
hTRa1	2.718006
hTRa1	2.326709
hTRa1	2.369932
CoA382PfsX7	2.383618
CoA382PfsX7	1.996378
CoA382PfsX7	2.340166
CoA382PfsX7	2.144127
CoA382PfsX7	2.156791
CoA382PfsX7	2.068286
CoA382PfsX7	2.09192
CoA382PfsX7	2.238431
CohTRa1	2.361562
CohTRa1	1.874758
CohTRa1	2.20944
CohTRa1	2.364252
CohTRa1	2.321375
CohTRa1	2.147228
CohTRa1	2.150043
CohTRa1	2.209673

Table 5: Chi-Square Observed Frequencies

	No aggregates	Aggregates	Total
Wild-type hTRα1	602	198	800
TRα1-A382PfsX7	640	160	800
Cotransfection (WT + Mutant)	373	327	700
Total	1615	685	2300